

Combining Smoothing Spline with Conditional Gaussian Graphical Model for Density and Graph Estimation

Runfei Luo, Anna Liu and Yuedong Wang *

February 2, 2022

Abstract

Multivariate density estimation and graphical models play important roles in statistical learning. The estimated density can be used to construct a graphical model that reveals conditional relationships whereas a graphical structure can be used to build models for density estimation. Our goal is to construct a consolidated framework that can perform both density and graph estimation. Denote \mathbf{Z} as the random vector of interest with density function $f(\mathbf{z})$. Splitting \mathbf{Z} into two parts, $\mathbf{Z} = (\mathbf{X}^T, \mathbf{Y}^T)^T$ and writing $f(\mathbf{z}) = f(\mathbf{x})f(\mathbf{y}|\mathbf{x})$ where $f(\mathbf{x})$ is the density function of \mathbf{X} and $f(\mathbf{y}|\mathbf{x})$ is the conditional density of $\mathbf{Y}|\mathbf{X} = \mathbf{x}$. We propose a semiparametric framework that models $f(\mathbf{x})$ nonparametrically using a smoothing spline ANOVA (SS ANOVA) model and $f(\mathbf{y}|\mathbf{x})$ parametrically using a conditional Gaussian graphical model (cGGM). Combining flexibility of the SS ANOVA model with succinctness of the cGGM, this framework allows us to deal with

*Runfei Luo (email: rluo@pstat.ucsb.edu) received her Ph.D. in statistics from University of California, Santa Barbara. She is now an applied scientist in Amazon Web Services. Anna Liu (email: anna@math.umass.edu) is Associate Professor, Department of Mathematics and Statistics, University of Massachusetts, Amherst, Massachusetts 01002., Yuedong Wang (email: yuedong@pstat.ucsb.edu) is Professor, Department of Statistics and Applied Probability, University of California, Santa Barbara, California 93106. Anna Liu's research was supported by a grant from the National Science Foundation (DMS-1507078). Runfei Luo and Yuedong Wang's research was supported by a grant from the National Science Foundation (DMS-1507620). We acknowledge support from the Center for Scientific Computing from the CNSI, MRL: an NSF MRSEC (DMR-1720256) for their support. Address for correspondence: Yuedong Wang, Department of Statistics and Applied Probability, University of California, Santa Barbara, California 93106.

high-dimensional data without assuming a joint Gaussian distribution. We propose a backfitting estimation procedure for the cGGM with a computationally efficient approach for selection of tuning parameters. We also develop a geometric inference approach for edge selection. We establish asymptotic convergence properties for both the parameter and density estimation. The performance of the proposed method is evaluated through extensive simulation studies and two real data applications.

KEY WORDS: cross-validation, high dimensional data, penalized likelihood, reproducing kernel Hilbert space, smoothing spline ANOVA

1 Introduction

Density estimation has long been a subject of paramount interest in statistics. Many parametric, nonparametric, and semiparametric methods have been developed in the literature. Assuming a known distribution family with succinct representation and interpretable parameters, the parametric approach is in general statistically and computationally efficient (Kendall, Stuart & Ord 1987). However, the parametric assumption may be too restrictive for some applications. The nonparametric approach, on the other hand, does not assume a specific form for the density function and allows its shape to be decided by data. Methods such as kernel estimation (Parzen 1962, Silverman 2018), local likelihood estimators (Loader 1996), and smoothing splines (Gu 2013) work well for low dimensional multivariate density functions. When the dimension is moderate to large, existing nonparametric methods break down quickly due to the curse of dimensionality and/or computational limitations. Duong (2007) pointed out that the kernel density estimation is not applicable to random variables of dimension higher than six. To reduce the computational burden, Jeon & Lin (2006) and Gu, Jeon & Lin (2013) developed pseudo likelihood method for smoothing spline density estimation. However, our experience indicates that the computation become almost infeasible when the dimension is higher than twelve. Consequently, contrary to the univariate case, flexible methods for multivariate density estimation are rather limited when the dimension is large. Recent work using piecewise constant and Bayesian partitions represents a major breakthrough in this area (Lu, Jiang & Wong 2013, Liu & Wong 2014, Li, Yang & Wong 2016). Nevertheless, these methods can handle moderate dimensions only, lead to non-

smooth density estimates, and cannot be used to investigate the conditional relationship.

Some semiparametric methods have been proposed to take advantage of the parsimony of parametric models and the flexibility of nonparametric modeling. Semiparametric copula models consist of nonparametric marginal distributions and parametric copula functions (Genest, Ghoudi & Rivest 1995). Projection pursuit density estimation overcomes the curse of dimensionality by representing the joint density as a product of some smooth univariate functions of carefully selected linear combinations of variables (Friedman, Stuetzle & Schroeder 1984). The regularized derivative expectation operator (rodeo) method assumes the joint density equals a product of a parametric component and a nonparametric function of an unknown subset of variables (Liu, Lafferty & Wasserman 2007). Other semiparametric/nonparametric methods for density estimation include mixture models (Richardson & Green 1997), forest density (Liu, Xu, Gu, Gupta, Lafferty & Wasserman 2011), density tree (Ram & Gray 2011), and geometric density estimation (Wang, Canale & Dunson 2016). All existing semiparametric/nonparametric methods have strengths and limitations. We will develop a new semiparametric procedure for multivariate density estimation that explores the sparse graph structure in the parametric part of the model.

Graphical models are used to characterize conditional relationship between variables with a wide range of applications in natural sciences, social sciences, and economics (Lauritzen 1996, Fan, Liao & Liu 2016, Friedman, Hastie & Tibshirani 2008). Gaussian graphical model (GGM) is one of the most popular models where conditional independence is reflected in the zero entries of the precision matrix (Friedman et al. 2008). The resulting structure from a GGM can be erroneous when the true distribution is far from Gaussian. The dependence structure of non-Gaussian data has not received great attention until recent years. Robustified Gaussian and elliptical graphical models against possible outliers were studied by Miyamura & Kano (2006), Finegold & Drton (2011), Vogel & Fried (2011), and Sun & Li (2012). Graphical models based on generalized linear models were proposed by Lee, Ganapathi & Koller (2007), Höfling & Tibshirani (2009), Ravikumar, Wainwright & Lafferty (2010), Allen & Liu (2012), and Yang, Allen, Liu & Ravikumar (2012). Nonparametric and semiparametric approaches have also been considered. Jeon & Lin (2006) and Gu et al. (2013) applied SS ANOVA density models to estimate graphs (see Section 3 for details). The computation of this nonparametric

approach becomes prohibitive for large dimensions. Liu, Lafferty & Wasserman (2009), Liu, Han, Yuan, Lafferty & Wasserman (2012), and Xue & Zou (2012) developed an elegant nonparanormal model which assumes that there exists a monotone transformation to each variable such that the joint distribution after transformation is multivariate Gaussian. Then any established estimation methods for the GGM can be applied to the transformed variables. Other semiparametric/nonparametric methods include graphical random forests (Fellinghauer, Bühlmann, Ryffel, Von Rhein & Reinhardt 2013), regularized score matching (Lin 2018), and kernel partial correlation (Oh 2017).

The goal of this article is to build a semiparametric model that combines the GGM with the SS ANOVA density model. We are interested in both density and graph estimation. The remainder of the article is organized as follows. In Section 2 we introduce the semiparametric density model and methods for estimation and computation. We propose methods for graph estimation in Section 3. Section 4 presents theoretical properties of our methods in term of both density and graph estimation. In Section 5 we evaluate our method using simulation studies. In Section 6 we present applications to two real datasets. Some technical details are gathered in the Appendix.

2 Density Estimation with SS ANOVA and cGGM

2.1 Semiparametric Density Models with SS ANOVA and cGGM

Consider the density estimation problem in which we are given a random sample of a random vector \mathbf{Z} , and we wish to estimate the density function $f(\mathbf{z})$ of \mathbf{Z} . Let $\mathbf{Z} = (\mathbf{X}^T, \mathbf{Y}^T)^T$ where $\mathbf{X} = (X_1, \dots, X_d)^T$ is a d -dimensional random vector for which the density function will be modeled nonparametrically and $\mathbf{Y} = (Y_1, \dots, Y_p)^T \in \mathbb{R}^p$ collects elements for which the conditional density will be modeled parametrically. The joint density function $f(\mathbf{z})$ can be decomposed into two components:

$$f(\mathbf{z}) = f(\mathbf{x}, \mathbf{y}) = f(\mathbf{x})f(\mathbf{y}|\mathbf{x}). \quad (1)$$

We will model $f(\mathbf{x})$ and $f(\mathbf{y}|\mathbf{x})$ using SS ANOVA models and cGGMs respectively. We now provide details of these models.

Assume $\mathbf{X} \in \mathcal{X} = \mathcal{X}_1 \times \dots \times \mathcal{X}_d$ where $X_u \in \mathcal{X}_u$ which is an arbitrary set. To deal with the positivity

and unity constraints of a density function, we consider the logistic transform $f = e^\eta / \int_{\mathcal{X}} e^\eta d\mathbf{x}$ where $\eta(\mathbf{x})$ is referred to as the logistic density function (Gu 2013). We construct a model space for η using the tensor product of reproducing kernel Hilbert spaces (RKHS). The SS ANOVA decomposition of functions in the tensor product RKHS can be represented as

$$\eta(\mathbf{x}) = c + \sum_{k=1}^d \eta_k(x_k) + \sum_{k>l} \eta_{kl}(x_k, x_l) + \cdots + \eta_{1\dots d}(x_1, \dots, x_d), \quad (2)$$

where η_k 's are main effects, η_{kl} 's are two-way interactions, and the rest are higher order interactions involving more than two variables. Higher order interactions are often removed in (2) for more tractable estimation and inference. An SS ANOVA model for the logistic density function assumes that η belongs to an RKHS which contains a subset of components in the SS ANOVA decomposition (2). For a given SS ANOVA model, terms included in the model can be regrouped and the model space can be expressed as

$$\mathcal{H} = \mathcal{H}^0 \oplus \mathcal{H}^1 \oplus \cdots \oplus \mathcal{H}^w, \quad (3)$$

where \mathcal{H}^0 is a finite dimensional space collecting all functions that are not going to be penalized, and $\mathcal{H}^1, \dots, \mathcal{H}^w$ are orthogonal RKHS's with reproducing kernels (RK) R^v for $v = 1, \dots, w$. Details about the SS ANOVA model can be found in Gu (2013) and Wang (2011).

We assume a cGGM for $f(\mathbf{y}|\mathbf{x})$. Specifically, we assume that $\mathbf{Y}|\mathbf{X} = \mathbf{x} \sim \mathcal{N}(-\Lambda^{-1}\Theta^T\mathbf{x}, \Lambda^{-1})$ where Λ is a $p \times p$ precision matrix and Θ is a $d \times p$ matrix that parameterizes the conditional relationship between \mathbf{X} and \mathbf{Y} (Sohn & Kim 2012, Wytock & Kolter 2013, Yuan & Zhang 2014). We note that the negative log likelihood function is convex under this parameterization. An alternative assumption $\mathbf{Y}|\mathbf{X} = \mathbf{x} \sim \mathcal{N}(\Psi\mathbf{x}, \Lambda^{-1})$ (Yin & Li 2011) may be used to model the conditional density $f(\mathbf{y}|\mathbf{x})$ where the negative log likelihood function is biconvex in Ψ and Λ rather than jointly convex.

We will refer to the proposed semiparametric model as combined smoothing spline and conditional Gaussian graphical (cSScGG) model. The cSScGG model is closely related to the semiparametric kernel density estimation (SKDE) proposed by Hoti & Holmström (2004). The same decomposition in (1) was considered. Given an iid sample $\mathbf{Z}_i = (\mathbf{X}_i^T, \mathbf{Y}_i^T)^T$, $i = 1, \dots, n$, Hoti & Holmström (2004) estimated $f(\mathbf{x})$ using the kernel density, $\hat{f}(\mathbf{x}) = n^{-1} \sum_{i=1}^n K_{h_1}(\mathbf{x} - \mathbf{X}_i)$, and $f(\mathbf{y}|\mathbf{x})$ using the conditional Gaussian density with mean $\mu(\mathbf{x})$ and covariance $\Sigma(\mathbf{x})$. Specifically, they estimated

$\mu(\mathbf{x})$ and covariance $\Sigma(\mathbf{x})$ by $\hat{\mu}(\mathbf{x}) = \sum_{i=1}^n W_{h_2}(\mathbf{x} - \mathbf{X}_i) \mathbf{Y}_i$ and $\hat{\Sigma}(\mathbf{x}) = \sum_{i=1}^n W_{h_3}(\mathbf{x} - \mathbf{X}_i) (\mathbf{Y}_i - \hat{\mu}(\mathbf{x})) (\mathbf{Y}_i - \hat{\mu}(\mathbf{x}))^T$ respectively, where $K_h(\mathbf{x}) = h^{-d} K(\mathbf{x}/h)$, K is the symmetric Gaussian kernel function, $W_h(\mathbf{x} - \mathbf{X}_i) = K_h(\mathbf{x} - \mathbf{X}_i) / \sum_{j=1}^n K_h(\mathbf{x} - \mathbf{X}_j)$, and h_1, h_2 , and h_3 are bandwidths. Selection of bandwidths can be difficult and the estimation of conditional mean and covariance can be poor when the dimension of \mathbf{Y} is large. The authors focused on the classification problem. They set $W_{h_2}(\mathbf{x} - \mathbf{X}_i) = W_{h_3}(\mathbf{x} - \mathbf{X}_i) = 1/n$ in their simulations to make the computation feasible. Under these weights the estimated conditional density $f(\mathbf{y}|\mathbf{x})$ does not depend on \mathbf{x} at all. In contrast, we model $f(\mathbf{y}|\mathbf{x})$ using a cGGM which will allow us to explore sparsity in the conditional dependence structure. In addition, the domain \mathcal{X} in our model is an arbitrary set while the domain in the SKDE method is a subset of \mathbb{R}^d . While we focus on continuous \mathbf{X} in this paper, the discrete case is a natural extension of the current work.

2.2 Penalized Likelihood Estimation

A cSScGG model consists of three parameters: $\eta \in \mathcal{H}$ and matrices Λ and Θ where \mathcal{H} is an RKHS given in (3) and Λ is positive definite. Given an iid sample $\mathbf{Z}_i = (\mathbf{X}_i^T, \mathbf{Y}_i^T)^T$, $i = 1, \dots, n$, let $X = (\mathbf{X}_1, \dots, \mathbf{X}_n)^T$, $Y = (\mathbf{Y}_1, \dots, \mathbf{Y}_n)^T$, $S_{xx} = n^{-1} X^T X$, $S_{yy} = n^{-1} Y^T Y$, and $S_{xy} = n^{-1} X^T Y$. Denote

$$l_1(\eta) = \frac{1}{n} \sum_{i=1}^n e^{-\eta(\mathbf{X}_i)} + \int_{\mathcal{X}} \eta(\mathbf{x}) \rho(\mathbf{x}) d\mathbf{x}, \quad (4)$$

$$l_2(\Theta, \Lambda) = -\log |\Lambda| + \text{tr}(S_{yy} \Lambda + 2S_{xy}^T \Theta + \Lambda^{-1} \Theta^T S_{xx}^T \Theta) \quad (5)$$

as the negative log pseudo likelihood and negative log likelihood functions based on \mathbf{X} and \mathbf{Y} samples respectively, where some constants are ignored and ρ is a known density for the pseudo likelihood (Gu 2013). The function $l_1(\eta)$ is continuous, convex and Fréchet differentiable (Jeon & Lin 2006), and the function $l_2(\Theta, \Lambda)$ is jointly convex in Λ and Θ .

We estimate η , Λ and Θ as minimizers of the penalized likelihood:

$$\{\hat{\eta}, \hat{\Lambda}, \hat{\Theta}\} = \arg \min_{\eta \in \mathcal{H}, \Lambda \succ 0, \Theta} \left\{ \left[l_1(\eta) + \frac{\lambda_1}{2} J(\eta) \right] + \left[l_2(\Lambda, \Theta) + \lambda_2 \|\Lambda\|_{1,\text{off}} + \lambda_3 \|\Theta\|_1 \right] \right\}, \quad (6)$$

where J is a semi-norm in \mathcal{H} that penalizes departure from the null space \mathcal{H}^0 , $\|\cdot\|_1$ denotes the elementwise ℓ_1 -norm, $\|\cdot\|_{1,\text{off}}$ denotes the elementwise ℓ_1 -norm on off-diagonal entries, and $\Lambda \succ 0$

indicates positive definiteness of Λ . Together, $\|\Lambda\|_{1,\text{off}}$ and $\|\Theta\|_1$ encourage sparsity for the cGGM. We allow different tuning parameters for different penalties.

Note that the first part of the penalized likelihood depends on η only and the second part depends on Θ and Λ only. Therefore, we can compute the penalized likelihood estimates by solving two optimization problems separately:

$$\hat{\eta} = \arg \min_{\eta \in \mathcal{H}} \left\{ \frac{1}{n} \sum_{i=1}^n e^{-\eta(\mathbf{x}_i)} + \int_{\mathcal{X}} \eta(\mathbf{x}) \rho(\mathbf{x}) d\mathbf{x} + \frac{\lambda_1}{2} J(\eta) \right\}, \quad (7)$$

and

$$\{\hat{\Theta}, \hat{\Lambda}\} = \arg \min_{\Lambda > 0, \Theta} \left\{ -\log |\Lambda| + \text{tr}(S_{yy}\Lambda + 2S_{xy}^T\Theta + \Lambda^{-1}\Theta^T S_{xx}^T\Theta) + \lambda_2 \|\Lambda\|_{1,\text{off}} + \lambda_3 \|\Theta\|_1 \right\}. \quad (8)$$

As in Gu (2013), we approximate the solution of (7) by a linear combination of basis functions in \mathcal{H}^0 and a random subset of representers. Then the estimate $\hat{\eta}$ can be calculated using the Newton-Raphson algorithm. The smoothing parameter λ_1 is selected as the minimizer of an approximated cross-validation estimate of the Kullback-Leibler (KL) divergence. Details can be found in Gu (2013), Gu et al. (2013), and Luo (2018). In the next section we propose a new computational method for solving (8).

2.3 Backfitting Algorithm for cGGM

Instead of updating Λ and Θ simultaneously as in Sohn & Kim (2012), Wytock & Kolter (2013) and Yuan & Zhang (2014), we will consider a backfitting procedure to update them iteratively until convergence. We use the subscript (t) to denote quantities calculated at iteration t and A_{ij} to denote the (i, j) -th element of a matrix A .

At iteration $t+1$, with Λ being fixed at $\Lambda_{(t)}$, (8) reduces to the minimization of a quadratic function plus an ℓ_1 penalty. Therefore, without needing to calculate the Hessian matrix, Θ can be updated efficiently using the coordinate descent algorithm. The gradient $\nabla_{\Theta} l_2(\Lambda, \Theta) = 2S_{xy} + 2S_{xx}\Theta\Lambda^{-1}$. Denote $\Sigma = \Lambda^{-1}$ as the covariance matrix. Then the (i, j) th element Θ_{ij} is updated by

$$\Theta_{ij,(t+1)} \leftarrow S_{\lambda_3/a_{\Theta}} \left(c_{\Theta} - \frac{b_{\Theta}}{a_{\Theta}} \right), \quad (9)$$

where $a_\Theta = 2\Sigma_{jj,(t)}(S_{xx})_{ii}$, $b_\Theta = 2(S_{xy})_{ij} + 2(S_{xx}\Theta_{(t)}\Sigma_{(t)})_{ij}$, $c_\Theta = \Theta_{ij,(t)}$, and $S_\omega(x) = \text{sign}(x) \max(|x| - \omega, 0)$ is the soft-thresholding operator with threshold ω .

To update Λ at iteration $t+1$, we consider the approximate conditional distribution $N(-\Lambda_{(t)}^{-1}\Theta_{(t)}^T\mathbf{x}, \Lambda^{-1})$ where both Θ and Λ in the conditional mean are fixed at their estimates from the t -th iteration. The resulting negative log likelihood

$$h_{(t)}(\Lambda) = -\log |\Lambda| + \text{tr}(S_{yy}\Lambda + 2S_{xy}^T\Theta_{(t)}\Lambda_{(t)}^{-1}\Lambda + \Lambda_{(t)}^{-1}\Lambda\Lambda_{(t)}^{-1}\Theta_{(t)}^T S_{xx}\Theta_{(t)}) \quad (10)$$

where terms independent of Λ are dropped. We update Λ by

$$\Lambda_{(t+1)} = \arg \min_{\Lambda > 0} \left\{ h_{(t)}(\Lambda) + \lambda_2 \|\Lambda\|_{1,\text{off}} \right\}. \quad (11)$$

As in Hsieh, Dhillon, Ravikumar & Sustik (2011), we will find the Newton direction by approximating $h_{(t)}$ using a quadratic function. Based on the second-order Taylor expansion of $h_{(t)}(\Lambda)$ at $\Lambda_{(t)}$ where $\Lambda = \Lambda_{(t)} + \Delta_\Lambda$ and ignoring terms independent of Δ_Λ , we consider

$$\bar{h}_{(t)}(\Delta_\Lambda) = \text{vec}(\nabla h_{(t)}(\Lambda_{(t)}))^T \text{vec}(\Delta_\Lambda) + \frac{1}{2} \text{vec}(\Delta_\Lambda)^T \nabla^2 h_{(t)}(\Lambda_{(t)}) \text{vec}(\Delta_\Lambda),$$

where $\nabla h_{(t)}(\Lambda_{(t)}) = S_{yy} + \Sigma_{(t)}\Theta_{(t)}^T S_{xx}\Theta_{(t)}\Sigma_{(t)} + 2\Sigma_{(t)}\Theta_{(t)}^T S_{xy} - \Sigma_{(t)}$ and $\nabla^2 h_{(t)}(\Lambda_{(t)}) = \Sigma_{(t)} \otimes \Sigma_{(t)}$ are gradient and Hessian matrices with respect to Λ respectively, and \otimes represents the Kronecker product. The Newton direction $D_{\Lambda,(t)}$ for (11) can be written as the solution of the following regularized quadratic function (Hsieh et al. 2011)

$$D_{\Lambda,(t)} = \arg \min_{\Delta_\Lambda} \left\{ \bar{h}_{(t)}(\Delta_\Lambda) + \lambda_2 \|\Lambda_{(t)} + \Delta_\Lambda\|_{1,\text{off}} \right\}. \quad (12)$$

Equation (12) can be solved efficiently via the coordinate descent algorithm. Specifically, let $\Delta_{\Lambda,(0)} = 0$ be the initial value, and $\Delta_{\Lambda,(s)}$ be the update at iteration s . Then at iteration $s+1$, the (i, j) th element of $\Delta_{\Lambda,(s)}$ is updated by

$$(\Delta_\Lambda)_{ij,(s+1)} \leftarrow (\Delta_\Lambda)_{ij,(s)} - c_\Lambda + S_{\lambda_2/a_\Lambda} \left(c_\Lambda - \frac{b_\Lambda}{a_\Lambda} \right), \quad (13)$$

where $a_\Lambda = \Sigma_{ij,(t)}^2 + \Sigma_{ii,(t)}\Sigma_{jj,(t)}$, $b_\Lambda = (S_{yy})_{ij} + \left(\Sigma_{(t)}\Theta_{(t)}^T S_{xx}\Theta_{(t)}\Sigma_{(t)} \right)_{ij} + 2 \left(\Sigma_{(t)}\Theta_{(t)}^T S_{xy} \right)_{ij} - \Sigma_{ij,(t)} + \left(\Sigma_{(t)}\Delta_{\Lambda,(s)}\Sigma_{(t)} \right)_{ij}$ and $c_\Lambda = \Lambda_{ij,(t)} + (\Delta_\Lambda)_{ij,(s)}$. Denote the penalized objective function at the t -th iteration as $p_{(t)}(\Lambda) \triangleq h_{(t)}(\Lambda) + \lambda_2 \|\Lambda\|_{1,\text{off}}$. We adopt the Armijo's rule (Armijo 1966) to find the step

size α . Specifically, with a constant decrease rate $0 < \beta < 1$ (typically $\beta = 0.5$), step sizes $\alpha = \beta^k$ for $k \in \mathbb{N}$ are tried until the smallest k such that

$$p_{(t)}(\Lambda_{(t)} + \alpha D_{\Lambda,(t)}) \leq p_{(t)}(\Lambda_{(t)}) + \alpha \sigma \left\{ \text{tr}(\nabla h_{(t)}(\Lambda_{(t)}) D_{\Lambda,(t)}) + \lambda_2 \|\Lambda_{(t)} + D_{\Lambda,(t)}\|_{1,\text{off}} - \lambda_2 \|\Lambda_{(t)}\|_{1,\text{off}} \right\},$$

where $0 < \sigma < 0.5$ is the backtracking termination threshold. After the step size is calculated, we update $\Lambda_{(t+1)} = \Lambda_{(t)} + \alpha D_{\Lambda,(t)}$.

When $n > \max(p, d)$, we use the maximum likelihood estimates $\check{\Lambda} = (S_{yy} - S_{xy}^T S_{xx}^{-1} S_{xy})^{-1}$ and $\check{\Theta} = -S_{xx}^{-1} S_{xy} \check{\Lambda}$ of Λ and Θ as initial values for Λ and Θ respectively (Yin & Li 2011). In the high dimensional case when S_{xx} is not invertible, we use the identity and zero matrix as initial values for Λ and Θ respectively.

The regularized Newton step (12) via the coordinate descent algorithm described above is the most computational expansive part of the algorithm. Despite its efficiency for lasso type of problems, updating all $p(p+1)/2$ variables in Λ is costly. To relieve this problem, we divide the parameter set into an active set and a free set. As in Hsieh et al. (2011) and Wytock & Kolter (2013), at the t th iteration of the algorithm, we only update Θ and Λ over the active set defined by

$$\begin{aligned} \mathcal{S}_{\Theta} &= \{(i, j) : |(\nabla_{\Theta} l_2(\Lambda_{(t)}, \Theta_{(t)}))_{ij}| > \lambda_3 \text{ or } \Theta_{ij,(t)} \neq 0\}, \\ \mathcal{S}_{\Lambda} &= \{(i, j) : |(\nabla h_{(t)}(\Lambda_{(t)}))_{ij}| > \lambda_2 \text{ or } \Lambda_{ij,(t)} \neq 0\}. \end{aligned} \tag{14}$$

As the active set is relatively small due to sparsity induced by the ℓ_1 regularization, this strategy provides a substantial speedup.

Tuning parameters λ_2 and λ_3 determine the sparsity of Λ and Θ . As a general selection tool, leave-one-out or k -fold cross-validation can be used to select these tuning parameters. The leave-one-out cross-validation (LOOCV) can be computationally intensive and various approximations have been proposed in the literature. Lian (2011) and Vujačić, Abbruzzo & Wit (2015) derived generalized approximate cross-validation (GACV) scores for selecting a single tuning parameter in the GGM. The BIC and k -fold CV have been used to select a single tuning parameter in the cGGM (Yin & Li 2011, Sohn & Kim 2012, Wytock & Kolter 2013, Yuan & Zhang 2014, Lee & Liu 2012). LOOCV has not been used for the cGGM as it requires fitting the model n times which is computationally intensive. To the best of our knowledge, there are no computationally efficient alternatives to LOOCV

in the current cGGM literature. We propose a new criterion, Leave-One-Out KL (LOOKL), for selecting λ_2 and λ_3 involved in (8) as minimizers of

$$\begin{aligned} & \text{LOOKL}(\lambda_2, \lambda_3) \\ &= -\frac{1}{n} l_2(\hat{\Lambda}, \hat{\Theta}) + \frac{1}{2n} \sum_{k=1}^n \left\{ \mathbf{u}_k^T (-C + B^T A^{-1} B)^{-1} [(-E + B^T A^{-1} D) \mathbf{v}_{xx,k} + 2B^T A^{-1} \mathbf{v}_{xy,k} - \mathbf{v}_{yy,k}] \right. \\ & \quad \left. + \mathbf{w}_k^T (-A + BC^{-1} B^T)^{-1} [(D - BC^{-1} E) \mathbf{v}_{xx,k} + BC^{-1} \mathbf{v}_{yy,k} - 2\mathbf{v}_{xy,k}] \right\}, \end{aligned} \quad (15)$$

where $S_{xx,k} = \mathbf{X}_k^T \mathbf{X}_k$, $S_{yy,k} = \mathbf{Y}_k^T \mathbf{Y}_k$, $S_{xy,k} = \mathbf{Y}_k^T \mathbf{X}_k$, $S_{xx}^{(-k)} = 1/n \sum_{i \neq k} S_{xx,i}$, $S_{yy}^{(-k)} = 1/n \sum_{i \neq k} S_{yy,i}$, $S_{xy}^{(-k)} = 1/n \sum_{i \neq k} S_{xy,i}$, $\mathbf{u}_k = \text{vec}(\hat{\Lambda}^{-1} - S_{yy,k} + \hat{\Lambda}^{-1} \hat{\Theta}^T S_{xx,k} \hat{\Theta} \hat{\Lambda}^{-1})$, $\mathbf{v}_{xx,k} = \text{vec}(S_{xx}^{(-k)} - S_{xx})$, $\mathbf{v}_{yy,k} = \text{vec}(S_{yy}^{(-k)} - S_{yy})$, $\mathbf{v}_{xy,k} = \text{vec}(S_{xy}^{(-k)} - S_{xy})$, $\mathbf{w}_k = \text{vec}(-2S_{xy,k} - 2S_{xx,k} \hat{\Theta} \hat{\Lambda}^{-1})$, $A = -2\hat{\Lambda}^{-1} \otimes S_{xx}$, $B = 2\hat{\Lambda}^{-1} \otimes S_{xx} \hat{\Theta} \hat{\Lambda}^{-1}$, $C = -\hat{\Lambda}^{-1} \otimes (\hat{\Lambda}^{-1} + 2\hat{\Lambda}^{-1} \hat{\Theta}^T S_{xx} \hat{\Theta} \hat{\Lambda}^{-1})$, $D = -2\hat{\Lambda}^{-1} \hat{\Theta}^T \otimes I_{d \times d}$, and $E = \hat{\Lambda}^{-1} \hat{\Theta}^T \otimes \hat{\Lambda}^{-1} \hat{\Theta}^T$. The derivation is deferred to Appendix A. Note that the GACV in Lian (2011) and KLCV in Vujačić et al. (2015) are special cases of LOOKL with $\Theta = 0$. In the penalized case, we ignored the partial derivatives corresponding to the zero elements in Θ and Λ Lian (2011), and showed that the LOOKL score remains the same. More details can be found in Luo (2018). Therefore, we conjecture that the proposed score is more appropriate for density estimation, rather than model selection.

We note the proposed backfitting procedure and LOOKL method for selecting tuning parameters are new for the cGMM. When Θ and Λ are simultaneously updated using the second-order Taylor expansion over all parameters (Wytock & Kolter 2013), an expensive computation of the large Hessian matrix of size $(p+d) \times (p+d)$ is required in each iteration. In contrast, our approach forms a second-order approximation of a function of Λ which requires a Hessian matrix of size $p \times p$. The remaining set of parameters in Θ can be updated easily using the simple coordinate descent algorithm. Moreover, compared to the method in McCarter & Kim (2016), our backfitting algorithm eliminates the need for computing the large matrix $\Sigma \Theta^T S_{xx} \Theta \Sigma$ in $\mathcal{O}(npd + np^2)$ time. Note that we always require Λ to be positive-definite after each iteration, so the algorithm still has complexity $\mathcal{O}(p^3)$ flops due to the Cholesky factorization.

Some off-the-shelf packages are utilized to solve the optimization problem. Specifically, we use

QUIC (Hsieh, Sustik, Dhillon & Ravikumar 2014) for updating Λ , and `gss` (Gu 2014) for computing the smoothing spline estimate of $f(\mathbf{x})$. We write R code for updating Θ using (9). We note that other penalties such as the smoothly clipped absolute deviation (SCAD) (Fan & Li 2001) and adaptive lasso (Zou 2006) may be used to replace the ℓ_1 penalty in the estimation of Θ and Λ . Details can be found in Luo (2018).

3 Graph Estimation with cSScGG Models

In Section 2 we proposed the cSScGG model as a flexible framework for estimating the multivariate density in high-dimensional setting. In terms of the graph structure, the edges among \mathbf{Y} are identified by $\hat{\Lambda}$, and edges between \mathbf{X} and \mathbf{Y} are identified by $\hat{\Theta}$ (Sohn & Kim 2012, Wytock & Kolter 2013, Yuan & Zhang 2014). The remaining task is the identification of conditional independence within \mathbf{X} variables which is the target of this section.

We have assumed that the model space for the logistic density η contains a subset of components in the SS ANOVA decomposition (2). The interactions are often truncated to overcome the curse of dimensionality and reduce the computational cost. As in Gu (2013) and Gu et al. (2013), in this section we consider the SS ANOVA model with all main effects and two-way interactions as the model space for η . We note that the SS ANOVA model allows pairwise nonparametric interactions as opposed to linear interactions in the GGM. Gu (2013) and Gu et al. (2013) proposed the squared error projection for assessing importance of each interaction term and subsequently identify edges. However, we cannot apply their method directly to $\hat{\eta}$ to identify edges within \mathbf{X} since the cGGM for $f(\mathbf{y}|\mathbf{x})$ also includes interaction terms among variables in \mathbf{X} .

The logarithm of the joint density

$$\begin{aligned} \log f(\mathbf{z}) &= \log f(\mathbf{x}) + \log f(\mathbf{y}|\mathbf{x}) \\ &= \eta(\mathbf{x}) + \frac{1}{2}(-\mathbf{y}^T \Lambda \mathbf{y} - 2\mathbf{x}^T \Theta \mathbf{y} - \mathbf{x}^T \Theta^T \Lambda^{-1} \Theta \mathbf{x}) + C, \end{aligned}$$

where C is a constant independent of \mathbf{x} and \mathbf{y} . The main challenge in identifying conditional independence among \mathbf{X} comes from the fact that $f(\mathbf{y}|\mathbf{x})$ brings in an extra term, $-\mathbf{x}^T \Theta^T \Lambda^{-1} \Theta \mathbf{x}/2$, into

the interactions among \mathbf{X} . Let

$$\hat{\zeta}(\mathbf{x}) = \hat{\Delta}(\mathbf{x}) + \hat{\eta}(\mathbf{x}). \quad (16)$$

where $\hat{\Delta}(\mathbf{x}) = -\mathbf{x}^T \hat{\Theta}^T \hat{\Lambda}^{-1} \hat{\Theta} \mathbf{x} / 2$. Define the functional

$$\tilde{V}(f, g) = \int_{\mathcal{X}} f(\mathbf{x}) g(\mathbf{x}) \rho(\mathbf{x}) d\mathbf{x} - \left\{ \int_{\mathcal{X}} f(\mathbf{x}) \rho(\mathbf{x}) d\mathbf{x} \right\} \left\{ \int_{\mathcal{X}} g(\mathbf{x}) \rho(\mathbf{x}) d\mathbf{x} \right\} \quad (17)$$

and denote $\tilde{V}(f, f)$ as $\tilde{V}(f)$. Let $\mathcal{H} = \mathcal{S}^0 \oplus \mathcal{S}^1$ where \mathcal{S}^1 collects functions whose contribution to the overall model is of question. The squared error projection of $\hat{\zeta}$ in \mathcal{S}^0 is (Gu 2013)

$$\tilde{\zeta} = \arg \min_{\zeta \in \mathcal{S}^0} \{ \tilde{V}(\hat{\zeta} - \zeta) \}. \quad (18)$$

$\tilde{V}(\hat{\zeta} - \zeta)$ can be regarded as a proxy of the symmetrized KL divergence (Gu 2013). Assuming $\zeta_u = -\log \rho(\mathbf{x}) \in \mathcal{S}^0$, it is easy to check that $\tilde{V}(\hat{\zeta} - \zeta_u) = \tilde{V}(\hat{\zeta} - \tilde{\zeta}) + \tilde{V}(\tilde{\zeta} - \zeta_u)$. Then the ratio $\tilde{V}(\hat{\zeta} - \tilde{\zeta}) / \tilde{V}(\hat{\zeta} - \zeta_u)$ reflects the importance of functions in \mathcal{S}^1 . The quantity $\tilde{V}(\hat{\zeta} - \zeta_u)$ is readily computable while details for computing the squared error projection $\tilde{\zeta}$ are given in Appendix B.

For any pair of variables X_i and X_j , consider the decomposition $\mathcal{H} = \mathcal{S}_{ij}^0 \oplus \mathcal{S}_{ij}^1$ where \mathcal{S}_{ij}^1 is the subspace consisting of two-way interactions between X_i and X_j , and \mathcal{S}_{ij}^0 contains all functions in \mathcal{H} except the two-way interactions between X_i and X_j . Note that $\zeta_{ij}(x_i, x_j) \triangleq \eta_{ij}(x_i, x_j) + \hat{\Delta}_{ij} x_i x_j \in \mathcal{S}_{ij}^1$ where $\hat{\Delta}_{ij} = (\hat{\Theta}^T \hat{\Lambda}^{-1} \hat{\Theta})_{ij}$. Compute the projection ratio $r_{ij} \triangleq \tilde{V}(\hat{\zeta} - \tilde{\zeta}) / \tilde{V}(\hat{\zeta} - \zeta_u)$ in which $\tilde{\zeta}$ is the squared error projection of $\hat{\zeta}$ in \mathcal{S}_{ij}^0 . The ratio r_{ij} indicates the importance of interactions between X_i and X_j , and we will add the interactions to the additive model sequentially according to the descending order of r_{ij} 's.

Consider the space decomposition $\mathcal{H} = \mathcal{S}^0 \oplus \mathcal{S}^1$. We start with \mathcal{S}^0 being the subspace spanned by all main effects. We calculate the projection ratio of $\hat{\zeta}$ in \mathcal{S}^0 as $r = \tilde{V}(\hat{\zeta} - \tilde{\zeta}) / \tilde{V}(\hat{\zeta} - \zeta_u)$ where $\tilde{\zeta}$ is the squared error projection in \mathcal{S}^0 . If r is larger than a threshold, \mathcal{S}^1 is deemed important and we move the interaction with the largest r_{ij} from \mathcal{S}^1 to \mathcal{S}^0 . We then calculate the projection ratio r with the updated \mathcal{S}^0 and \mathcal{S}^1 . The projection ratio decreases each time we move an interaction from \mathcal{S}^1 to \mathcal{S}^0 . Finally the process stops when r falls below a cut-off value, at which time we denote the corresponding \mathcal{S}^0 as \mathcal{S}_s^0 . Let $\Pi_{ij} = I(\zeta_{ij} \in \mathcal{S}_s^0)$ and remove the edge between X_i and X_j if $\Pi_{ij} = 0$. In our implementations, the cut-off value is set to be 3%.

To summarize, the conditional independences among \mathbf{Y} , between \mathbf{X} and \mathbf{Y} , and among \mathbf{X} are characterized by the zero elements in $\hat{\Lambda}$, $\hat{\Theta}$ and Π , respectively. The whole procedure for edge identification is illustrated in Figure 1.

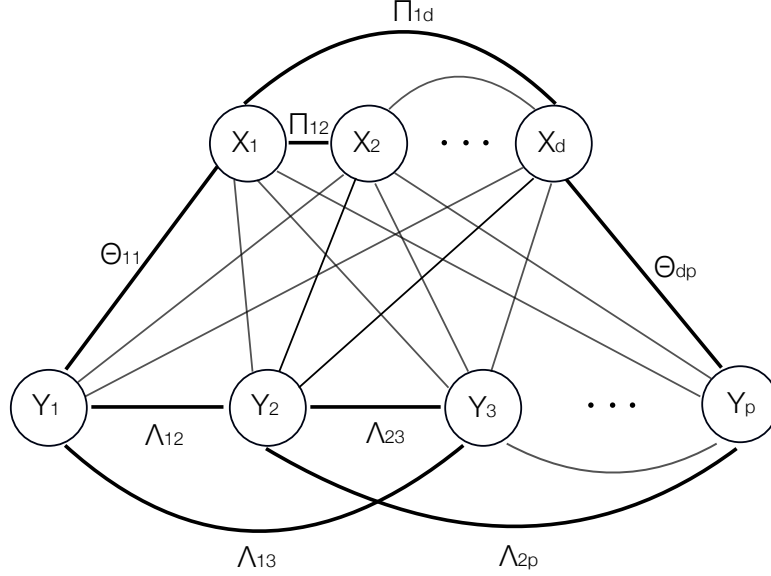


Figure 1: Illustration of the edge identification procedure.

4 Theoretical Analysis

We list notations, assumptions, and theoretical results only. Proofs are given in Appendix C.

4.1 Notations and Assumptions

Given a matrix U , let $\|U\|_2 = \sqrt{\lambda_{\max}(U^T U)}$, $\|U\|_\infty = \max_{i=1, \dots, p} \sum_{j=1}^p |U_{ij}|$ and $\|U\|_F = \sqrt{\sum_{i=1}^p \sum_{j=1}^p U_{ij}^2}$ denote the ℓ_2 operator norm, ℓ_∞ operator norm and Frobenius norm respectively, where $\lambda_{\max}(U^T U)$ represents the largest eigenvalue of $U^T U$. We assume that $\mathbf{Y}|\mathbf{X} = \mathbf{x} \sim \mathcal{N}(-\Lambda_0^{-1}\Theta_0^T \mathbf{x}, \Lambda_0^{-1})$ where Λ_0 and Θ_0 are the true parameters. Let $\Gamma_0 = (\Lambda_0^T, \Theta_0^T)^T$, $\Sigma_0 = \Lambda_0^{-1}$, $C_\sigma = \max_i \Sigma_{0,ii}$, $C_\Sigma = \max_{i,j} |\Sigma_{0,ij}|$, $C_\Theta = \max_{i,j} |\Theta_{0,ij}|$, $C_X = \max_{j=1, \dots, d} \|\mathbf{X}^j\|_2 / \sqrt{n}$ where \mathbf{X}^j is the j th columns of X , $H_0 = \nabla_{\Lambda, \Theta}^2 l_2(\Lambda_0, \Theta_0)$ denote the Hessian matrix evaluated at the true parameters, and $\kappa_H = \max_{i,j} |H_{0,ij}^{-1}|$. Let $\gamma = \max_{1 \leq j \leq p} \left\{ \sum_{i=1}^{d+p} I(\Gamma_{0,ij} \neq 0) \right\}$ be the maximum number of non-zeros in any

column of Γ_0 which represents the maximum degree of \mathbf{Y} in the graph.

Denote $\lambda = \max\{\lambda_2, \lambda_3\}$ and $r = \min\{\lambda_2, \lambda_3\}/\lambda$, then $r \leq 1$. In the following theoretical analysis, we assume that $\lambda_2 \geq \lambda_3$ and $r = \lambda_3/\lambda_2$. Similar arguments apply to the case of $\lambda_2 < \lambda_3$. The objective function can be rewritten as

$$\{\hat{\Theta}, \hat{\Lambda}\} = \arg \min_{\Lambda > 0, \Theta} \{l_2(\Lambda, \Theta) + \lambda(\|\Lambda\|_1 + r \|\Theta\|_1)\}. \quad (19)$$

We make the following assumptions.

Assumption 1. (*Underlying Model*) $\mathbf{Y}|\mathbf{X} = \mathbf{x} \sim N(-\Lambda_0^{-1}\Theta_0^T\mathbf{x}, \Lambda_0^{-1})$ where \mathbf{Y} has the maximum degree γ .

Assumption 2. (*Restricted Convexity*) For any $i = 1, \dots, p$, let S_i denote the nonzero indices of the i -th column of Θ_0 (i.e., the edges between \mathbf{X} and Y_i). We have $\lambda_{\min}(1/nX_{S_i}^T X_{S_i}) > 0$, where $\lambda_{\min}(\cdot)$ denotes the smallest eigenvalue and X_{S_i} represents the $n \times |S_i|$ matrix with columns of X indexed by S_i .

Assumption 3. (*Mutual incoherence*) Let S denote the support set of Γ_0 in vector form $S = (\text{vec}(\text{supp}\{\Lambda_0\})^T, \text{vec}(\text{supp}\{\Theta_0\})^T)^T$ where $\text{supp}\{\cdot\}$ denotes the indicator function of whether an element is zero. Let \bar{S} denote the complement of S . We have $\|H_{0, \bar{S}S}(H_{0, SS})^{-1}\|_{\infty} \leq 1 - \alpha$ for some $\alpha \in (0, 1)$, where $H_{0, \bar{S}S}$ and $H_{0, SS}$ represent the $|\bar{S}| \times |S|$ and $|S| \times |S|$ sub-matrices of H_0 with entries in $\bar{S} \times S$ and $S \times S$ respectively.

Assumption 4. (*Control of eigenvalues*) There exists some constants $0 < C_L \leq C_U < \infty$, such that $C_L \leq \lambda_{\min}(\Lambda_0) \leq \lambda_{\max}(\Lambda_0) \leq C_U$.

Assumption 1 provides the true underlying model. Assumption 2 ensures the solution of optimization problem (19) is restricted to the active set (nonzero entries in Λ_0 and Θ_0), which is also used in Wainwright (2009) and Wytock & Kolter (2013). Assumption 3 limits the influence of edges in inactive set (\bar{S}) can have on the edges in active set (S), and Assumption 4 bounds the eigenvalues of the precision matrix. Define $V(f, g) = \int_{\mathcal{X}} f(\mathbf{x})g(\mathbf{x})\rho(\mathbf{x})d\mathbf{x}$ and $V(f) = \int_{\mathcal{X}} f^2(\mathbf{x})\rho(\mathbf{x})d\mathbf{x}$.

Assumption 5. V is completely continuous with respect to J and $J(\eta_0) < \infty$.

Under the Assumption 5, there exists ϕ_ν such that $V(\phi_\nu, \phi_\mu) = \delta_{\nu,\mu}$, $J(\phi_\nu, \phi_\mu) = \rho_\nu \delta_{\nu,\mu}$, and $0 \leq \rho_\nu \uparrow \infty$, where $\delta_{\nu,\mu}$ is the Kronecker delta and ρ_ν is referred to as the eigenvalues of J with respect to V . Denote the Fourier series expansion of η_0 as $\eta_0 = \sum_\nu \eta_{\nu,0} \phi_\nu$ where $\eta_{\nu,0} = V(\eta_0, \phi_\nu)$ are the Fourier coefficients. Let $\tilde{\eta} = \sum_\nu \tilde{\eta}_\nu \phi_\nu$ where $\tilde{\eta}_\nu = (\beta_\nu + \eta_{\nu,0}) / (1 + \lambda_1 \rho_\nu)$ and $\beta_\nu = n^{-1} \sum_{i=1}^n \{e^{-\eta_0(\mathbf{X}_i)} \phi_\nu(\mathbf{X}_i) - \int_{\mathcal{X}} \phi_\nu(\mathbf{x}) \rho(\mathbf{x}) d\mathbf{x}\}$.

Assumption 6. (a) *The eigenvalues ρ_ν of J with respect to V satisfy $\rho_\nu > \beta \nu^s$ for some $\beta > 0$ and $s > 1$ when ν is sufficiently large.*

(b) *There exists some constants $0 < C_{1,1} < C_{1,2} < \infty$, $C_{1,3} < \infty$ and $C_{1,4} < \infty$ such that $C_{1,1} < e^{\eta_0(\mathbf{x}) - \eta(\mathbf{x})} < C_{1,2}$ holds uniformly for η in a convex set around η_0 containing $\hat{\eta}$ and $\tilde{\eta}$, $e^{-\eta_0(\mathbf{x})} < C_{1,3}$, and $\int_{\mathcal{X}} \phi_\nu^2(\mathbf{x}) \phi_\mu^2(\mathbf{x}) e^{-\eta_0(\mathbf{x})} \rho(\mathbf{x}) d\mathbf{x} < C_{1,4}$ for any ν and μ .*

(c) *There exists some $q \in [1, 2]$ such that $\sum_\nu \rho_\nu^q \eta_{\nu,0}^2 < \infty$.*

Assumptions 5 and 6 are commonly used in smoothing spline literatures to study the convergence rate for nonparametric density estimation (Gu 2013).

4.2 Asymptotic Consistency of the Estimated Parameters

The following theorem provides the estimation error bound and edge selection accuracy.

Theorem 1. *Suppose that the Assumptions 2 and 3 hold, $\tau > 2$, and n and $\lambda = \max\{\lambda_2, \lambda_3\}$ satisfy*

$$\begin{aligned} n &\geq C_{2,1} C_{2,2}^2 C_\sigma^2 \gamma^4 (1 + 8\alpha^{-1})^4 [\tau \log(pd) + \log 4], \\ \lambda &= 8\alpha^{-1} C_\sigma C_X^* \sqrt{3200} \sqrt{\frac{\tau \log(pd) + \log 4}{n}}, \end{aligned} \quad (20)$$

where $C_{2,1} = \max\{12800, 32C_X^2\}$, $C_{2,2} = \kappa_H \max\{3C_\Sigma/\gamma, 2/(C_\Theta\gamma), 412C_\Sigma^4 C_\Theta^2 C_X^2\}$, and $C_X^* = \max\{C_X^2, 1\}$, then with probability greater than $1 - (p^{-(\tau-2)} + (pd)^{-(\tau-1)})$, we have

1. *The estimates satisfy the elementwise ℓ_∞ bound:*

$$\max \left\{ \left\| \hat{\Lambda} - \Lambda_0 \right\|_\infty, \left\| \hat{\Theta} - \Theta_0 \right\|_\infty \right\} \leq 2\kappa_H (1 + 8\alpha^{-1}) C_\sigma C_X^* \sqrt{3200} \sqrt{\frac{\tau \log(pd) + \log 4}{n}}.$$

2. All non-zero entries of the solution $(\hat{\Lambda}, \hat{\Theta})$ are a subset of the non-zero entries of (Λ_0, Θ_0) .

Furthermore, non-zero entries of $(\hat{\Lambda}, \hat{\Theta})$ includes all non-zero entries (i, j) in (Λ_0, Θ_0) that satisfy

$$\min\{\Lambda_{0,ij}, \Theta_{0,ij}\} > 4\kappa_H(1 + 8\alpha^{-1})C_\sigma C_X^* \sqrt{3200} \sqrt{\frac{\tau \log(pd) + \log 4}{n}}. \quad (21)$$

Remark 1: i) Theorem 1 indicates that a sample size larger than a constant times $\gamma^4 \log(pd)$ is enough for our estimation procedure to identify a subset of the true non-zero elements in the cGGM, and the resulting estimations are close to the true parameters in ℓ_∞ bound. The convergence rate is the same as that in Wytock & Kolter (2013), but the success probability of the primal-dual witness approach as well as the exact bounds for n and λ are different. We also provide a lower bound for the sign consistency which is not included in Wytock & Kolter (2013).

ii) The convergence probability is smaller than that for the GGM (Wainwright 2009) where only a precision matrix needs to be estimated. This is the price we pay for estimating extra parameters in Θ .

Define s_Λ as the total number of non-zero elements in off-diagonal positions of Λ_0 , and s_Θ as the total number of non-zero elements in Θ_0 .

Corollary 1. *Under the same assumptions as in Theorem 1, with probability at least $1 - (p^{-(\tau-2)} + (pd)^{-(\tau-1)})$, the estimates $\hat{\Lambda}$ and $\hat{\Theta}$ satisfy*

$$\begin{aligned} & \max \left\{ \left\| \hat{\Lambda} - \Lambda_0 \right\|_F, \left\| \hat{\Theta} - \Theta_0 \right\|_F \right\} \\ & \leq 2\kappa_H(1 + 8\alpha^{-1}) \max\{\sqrt{p + s_\Lambda}, \sqrt{s_\Theta}\} C_\sigma C_X^* \sqrt{3200} \sqrt{\frac{\tau \log(pd) + \log 4}{n}}. \end{aligned} \quad (22)$$

Remark 2: The Frobenius norm was not studied in Wytock & Kolter (2013). We develop it as a building block for establishing the convergence rate for the density estimation in Section 4.3.

4.3 Convergence Rates for the Density Estimation

We first introduce a combined measure of divergence between the joint density and its estimate. Let $f_0(\mathbf{x}) = e^{\eta_0(\mathbf{x})} \rho(\mathbf{x}) / \int_{\mathcal{X}} e^{\eta_0(\mathbf{x})} \rho(\mathbf{x}) d\mathbf{x}$ and $f_0(\mathbf{y}|\mathbf{x})$ be the true densities of \mathbf{X} and $\mathbf{Y}|\mathbf{X} = \mathbf{x}$ with their

estimates denoted as $\hat{f}(\mathbf{x}) = e^{\hat{\eta}(\mathbf{x})}\rho(\mathbf{x})/\int_{\mathcal{X}}e^{\hat{\eta}(\mathbf{x})}\rho(\mathbf{x})d\mathbf{x}$ and $\hat{f}(\mathbf{y}|\mathbf{x})$ respectively. The KL divergence between two density functions f_1 and f_2 are defined as $\text{KL}(f_1, f_2) = \mathbb{E}_{f_1}[\log(f_1/f_2)]$. Then the symmetrized KL divergence between the true joint density $f_0(\mathbf{z}) = f_0(\mathbf{x})f_0(\mathbf{y}|\mathbf{x})$ and its estimate $\hat{f}(\mathbf{z}) = \hat{f}(\mathbf{x})\hat{f}(\mathbf{y}|\mathbf{x})$ can be expressed as

$$\begin{aligned}
& \text{SKL}(f_0(\mathbf{z}), \hat{f}(\mathbf{z})) \\
&= \text{KL}(f_0(\mathbf{z}), \hat{f}(\mathbf{z})) + \text{KL}(\hat{f}(\mathbf{z}), f_0(\mathbf{z})) \\
&= \left\{ \int_{\mathcal{X}} f_0(\mathbf{x})\text{KL}(f_0(\mathbf{y}|\mathbf{X}=\mathbf{x}), \hat{f}(\mathbf{y}|\mathbf{X}=\mathbf{x}))d\mathbf{x} + \int_{\mathcal{X}} \hat{f}(\mathbf{x})\text{KL}(\hat{f}(\mathbf{y}|\mathbf{X}=\mathbf{x}), f_0(\mathbf{y}|\mathbf{X}=\mathbf{x}))d\mathbf{x} \right\} \\
&+ \left\{ \text{KL}(f_0(\mathbf{x}), \hat{f}(\mathbf{x})) + \text{KL}(\hat{f}(\mathbf{x}), f_0(\mathbf{x})) \right\} \\
&\triangleq \text{SKL}(f_0(\mathbf{y}|\mathbf{x}), \hat{f}(\mathbf{y}|\mathbf{x})) + \text{SKL}(f_0(\mathbf{x}), \hat{f}(\mathbf{x})). \tag{23}
\end{aligned}$$

We will establish the asymptotic convergence rate under the following combined measure of divergence

$$D(f_0(\mathbf{z}), \hat{f}(\mathbf{z})) \triangleq \text{SKL}(f_0(\mathbf{y}|\mathbf{x}), \hat{f}(\mathbf{y}|\mathbf{x})) + (V + \lambda_1 J)(\eta_0 - \hat{\eta}). \tag{24}$$

The difference between (24) and (23) lies in the divergence measures for the estimation of $f(\mathbf{x})$. Note that the rate in $V(\eta - \eta_0)$ implies rate in $\tilde{V}(\eta - \eta_0)$, since $\tilde{V}(f) \leq V(f)$ and $\tilde{V}(\eta_0 - \hat{\eta})$ is a proxy of $\text{SKL}(f_0(\mathbf{x}), \hat{f}(\mathbf{x}))$ (Gu 2013).

We first establish the rate for $\text{SKL}(f_0(\mathbf{y}|\mathbf{x}), \hat{f}(\mathbf{y}|\mathbf{x}))$ which has the explicit expression:

$$\begin{aligned}
& \text{SKL}(f_0(\mathbf{y}|\mathbf{x}), \hat{f}(\mathbf{y}|\mathbf{x})) \\
&= \frac{1}{2}\mathbf{a}^T\hat{\Lambda}\mathbf{a} \int_{\mathcal{X}} \mathbf{x}^T\mathbf{x}f_0(\mathbf{x})d\mathbf{x} + \frac{1}{2}\mathbf{a}^T\Lambda_0\mathbf{a} \int_{\mathcal{X}} \mathbf{x}^T\mathbf{x}\hat{f}(\mathbf{x})d\mathbf{x} + \frac{1}{2}\text{tr}(\hat{\Lambda}^{-1}\Lambda_0 + \Lambda_0^{-1}\hat{\Lambda}) - p,
\end{aligned}$$

where $\mathbf{a} = \hat{\Lambda}^{-1}\hat{\Theta}^T - \Lambda_0^{-1}\Theta_0^T$. We assume that the second moments of marginal densities of f_0 and \hat{f} exist.

Theorem 2. *Under the Assumption 4 and conditional on the event $\left\| \hat{\Lambda} - \Lambda_0 \right\|_F \leq 0.5C_L$, we have*

$$\text{SKL}(f_0(\mathbf{y}|\mathbf{x}), \hat{f}(\mathbf{y}|\mathbf{x})) = \mathcal{O}\left(n^{-5/2}p^{5/2}(\log pd)^{5/2} + n^{-1}p^2(\log pd)\right). \tag{25}$$

For the smoothing spline ANOVA estimate $\hat{\eta}$ of η_0 , under the Assumptions 5 and 6, Gu (2013) showed that as $\lambda_1 \rightarrow 0$ and $n\lambda_1^{2/s} \rightarrow \infty$,

$$(V + \lambda_1 J)(\hat{\eta} - \eta_0) = \mathcal{O}(n^{-1}\lambda_1^{-1/s} + \lambda_1^q). \quad (26)$$

Finally, we have the convergence rate for the joint density estimate.

Theorem 3. *Suppose that the Assumptions 2-6 hold, $\tau > 2$, $\lambda_1 \rightarrow 0$, $n\lambda_1^{2/s} \rightarrow \infty$, and n and λ satisfy*

$$\begin{aligned} n &\geq C_{3,1}C_{3,2}^2C_\sigma^2 \max\{\gamma^4, p + s_\Lambda\}(1 + 8\alpha^{-1})^4[\tau \log(pd) + \log 4], \\ \lambda &= 8\alpha^{-1}C_\sigma C_X^* \sqrt{3200} \sqrt{\frac{\tau \log(pd) + \log 4}{n}}, \end{aligned} \quad (27)$$

where $C_{3,1} = C_{2,1} = \max\{12800, 32C_X^2\}$, and $C_{3,2} = \max\{C_{2,2}, \kappa_H \sqrt{1600}/C_L\} = \kappa_H \max\{3C_\Sigma/\gamma, 2/(C_\Theta\gamma), 412C_\Sigma^4 C_\Theta^2 C_X^2, \sqrt{1600}/C_L\}$, then with probability greater than $1 - (p^{-(\tau-2)} + (pd)^{-(\tau-1)})$ we have

$$D(f_0(\mathbf{z}), \hat{f}(\mathbf{z})) = \mathcal{O}(n^{-5/2}p^{5/2}(\log pd)^{5/2} + n^{-1}p^2(\log pd) + n^{-1}\lambda_1^{-1/s} + \lambda_1^q). \quad (28)$$

Remark 3: For low-dimensional \mathbf{X} (usually $d \leq 3$), the computation of multivariate integrals are feasible. We may use the penalized likelihood instead of the pseudo likelihood to estimate the density function $f(\mathbf{x})$. This leads to $f_0(\mathbf{x}) = e^{\eta_0} / \int_{\mathcal{X}} e^{\eta_0}$. Under similar conditions, Gu (2013) has proved that the symmetrized KL divergence $\text{SKL}(f_0(\mathbf{x}), \hat{f}(\mathbf{x}))$ is also $\mathcal{O}(n^{-1}\lambda_1^{-1/s} + \lambda_1^q)$, where $\hat{f}(\mathbf{x})$ is the penalized likelihood estimate. If we also use the penalized likelihood to estimate η in our model, then $\text{SKL}(f_0(\mathbf{z}), \hat{f}(\mathbf{z})) = \mathcal{O}(n^{-5/2}p^{5/2}(\log pd)^{5/2} + n^{-1}p^2(\log pd) + n^{-1}\lambda_1^{-1/s} + \lambda_1^q)$.

5 Simulation Studies

We have conducted extensive simulation experiments to evaluate the performance of the cSScGG procedure, and compare it with some existing parametric and semiparametric/nonparametric methods. To save space, we present some simulation results and more comprehensive results can be found in Luo (2018). We note that the cSScGG method can outperform the maximum likelihood estimation

(MLE) when $\mathbf{Z} = (\mathbf{X}^T, \mathbf{Y}^T)^T$ is multivariate Gaussian and the cGGM for \mathbf{Y} is sparse. Results for density and graph estimations are presented in Sections 5.1 and 5.2 respectively.

For density estimation, we use both LOOKL and CV (5-fold) methods to choose λ_2 and λ_3 . Tuning parameters involved in all other methods are chosen by 5-fold CV. For graph estimation, we select λ_2 and λ_3 in the cSScGG method as minimizers of the following BIC score

$$\text{BIC}(\lambda_2, \lambda_3) = \left\{ -n \log |\hat{\Lambda}| + n \text{tr}(S_{yy} \hat{\Lambda} + 2S_{xy}^T \hat{\Theta} + \hat{\Lambda}^{-1} \hat{\Theta}^T S_{xx} \hat{\Theta}) \right\} + \log n \{ \xi(\hat{\Lambda})/2 + \xi(\hat{\Theta}) \}, \quad (29)$$

where $\xi(\hat{\Lambda})$ and $\xi(\hat{\Theta})$ are the number of non-zero off-diagonal elements in $\hat{\Lambda}$ and the number of non-zero elements in $\hat{\Theta}$ respectively. The degree of freedom is defined in the same way as in Yin & Li (2011). The BIC is also used to select tuning parameters in other methods for graph estimation. More details regarding comparison of various tuning parameter selection methods are included in Luo (2018).

5.1 Density Estimation

We set $n = 200$, $d = 3$, and $p = 25$. We generate $\mathbf{X} \sim \omega \mathcal{N}(\boldsymbol{\mu}_1, \sigma^2 I) + (1 - \omega) \mathcal{N}(\boldsymbol{\mu}_2, \sigma^2 I)$ with $\boldsymbol{\mu}_1 = (1, 0, -1)^T$, and $\boldsymbol{\mu}_2 = (0, -1, 1)^T$. We consider four combinations of σ and ω : $\sigma = 0.5, 0.1$ and $\omega = 0.9, 0.1$. All results are reported based on 100 replications under each setting. In each replication, we first generate n iid samples $\mathbf{X}_1, \dots, \mathbf{X}_n$ from the multivariate Gaussian mixtures, then \mathbf{Y}_i 's are generated from a cGGM. Specifically, we randomly create a $(d+p) \times (d+p)$ precision matrix Ω using the R-package `huge` (Zhao, Liu, Roeder, Lafferty & Wasserman 2012), in which the probability of the off-diagonal elements being nonzero equals 0.2. The decomposition $\Omega = \begin{bmatrix} \Omega_{xx} & \Omega_{xy} \\ \Omega_{yx} & \Omega_{yy} \end{bmatrix}$ gives us $\Theta = \Omega_{xy}$ and $\Lambda = \Omega_{yy}$ (Yuan & Zhang 2014), so that we can sample \mathbf{Y}_i from $\mathcal{N}(-\Lambda^{-1} \Theta^T \mathbf{X}_i, \Lambda^{-1})$ for $i = 1, \dots, n$.

Since the division of non-Gaussian variables \mathbf{X} and Gaussian variables \mathbf{Y} is typically unknown in practice, we consider two versions of the proposed method – plain cSScGG and cSScGG with normality test (denoted as NT). In the plain version, we assume that the true non-Gaussian components are known and apply cSScGG directly. In the NT version, we select d variables with smallest p-values based on the Shapiro-Wilk test to all $p + d$ marginal variables as \mathbf{X} , and then apply the cSScGG

method.

In addition to the cSScGG method, we estimate density using the SKDE (Hoti & Holmström 2004), MLE, and QUIC (Hsieh et al. 2011) methods. In the implementation of the SKDE method, we use the R-package `ks` (Duong 2007) to calculate the kernel density estimate for $f(\mathbf{x})$ with the bandwidth selected by the smoothed cross-validation selector with diagonal bandwidth matrices (`Hscv.diag(x)`) which provides the best overall performance. To avoid selecting the two extra bandwidths involved in SKDE, as in Hoti & Holmström (2004), we set $f(\mathbf{y}|\mathbf{x}) = f(\mathbf{y})$ and use MLE to estimate $f(\mathbf{y})$. MLE and QUIC methods treat $\mathbf{Z}^T = (\mathbf{X}^T, \mathbf{Y}^T)$ as multivariate normal across all settings, and the estimates from these two methods are further broken down into $f(\mathbf{x})$ and $f(\mathbf{y}|\mathbf{x})$ for comparison. Specifically, QUIC method learns the precision matrix of \mathbf{Z} by forming a quadratic approximation of the log-likelihood, and the estimates are computed using the R-package QUIC (Hsieh et al. 2014). To evaluate the performance of different methods, we consider the KL divergence between the estimated density and the true density

$$\text{KL}(f_0(\mathbf{z}), \hat{f}(\mathbf{z})) = \mathbb{E}_{\mathbf{X}} \left[\text{KL}(f_0(\mathbf{y}|\mathbf{X}), \hat{f}(\mathbf{y}|\mathbf{X})) \right] + \text{KL}(f_0(\mathbf{x}), \hat{f}(\mathbf{x})),$$

where f_0 is the true density, and the aggregated KL $\mathbb{E}_{\mathbf{X}} \left[\text{KL}(f_0(\mathbf{y}|\mathbf{X}), \hat{f}(\mathbf{y}|\mathbf{X})) \right]$ is approximated by the empirical aggregated KL divergence. Table 1 reports the overall KL divergence $\text{KL}(f_0(\mathbf{z}), \hat{f}(\mathbf{z}))$, the empirical aggregated KL divergence $n^{-1} \sum_{i=1}^n \text{KL}(f_0(\mathbf{y}|\mathbf{X}_i), \hat{f}(\mathbf{y}|\mathbf{X}_i))$, and $\text{KL}(f_0(\mathbf{x}), \hat{f}(\mathbf{x}))$. They provide evaluations for the estimation of $f(\mathbf{z})$, $f(\mathbf{y}|\mathbf{x})$, and $f(\mathbf{x})$, respectively.

KL	Method	$\sigma = 0.5$	$\sigma = 0.5$	$\sigma = 0.1$	$\sigma = 0.1$
		$\omega = 0.9$	$\omega = 0.5$	$\omega = 0.9$	$\omega = 0.5$
$f(\mathbf{x})$	cSScGG	0.030 (0.023)	0.043 (0.021)	0.062 (0.073)	0.046 (0.026)
	SKDE	0.208 (0.172)	0.181 (0.190)	0.503 (0.414)	0.141 (0.091)
	QUIC	0.225 (0.023)	0.243 (0.012)	3.313 (0.051)	3.528 (0.021)
	MLE	0.182 (0.021)	0.225 (0.010)	3.128 (0.047)	3.487 (0.023)
$f(\mathbf{y} \mathbf{x})$	cSScGG_CV	1.145 (0.202)	1.118 (0.189)	1.040 (0.138)	1.078 (0.175)
	cSScGG_LOOKL	1.143 (0.164)	1.098 (0.167)	1.14 (0.172)	1.112 (0.161)
	SKDE	1.621 (0.184)	1.632 (0.218)	1.425 (0.173)	1.474 (0.215)
	QUIC	1.196 (0.125)	1.163 (0.147)	1.179 (0.141)	1.156 (0.139)
	MLE	1.827 (0.245)	1.613 (0.236)	2.235 (0.413)	1.607 (0.235)
$f(\mathbf{z})$	cSScGG_CV	1.175 (0.205)	1.161 (0.189)	1.102 (0.155)	1.124 (0.178)
	cSScGG_CV_NT	1.262 (0.208)	1.268 (0.173)	1.032 (0.125)	1.051 (0.120)
	cSScGG_LOOKL	1.173 (0.167)	1.141 (0.166)	1.202 (0.186)	1.158 (0.164)
	cSScGG_LOOKL_NT	1.358 (0.241)	1.325 (0.211)	1.153 (0.184)	1.122 (0.166)
	SKDE	1.829 (0.256)	1.813 (0.331)	1.928 (0.455)	1.615 (0.234)
	QUIC	1.422 (0.132)	1.405 (0.148)	4.492 (0.15)	4.684 (0.137)
	MLE	2.009 (0.245)	1.838 (0.237)	5.363 (0.404)	5.094 (0.232)

Table 1: Averages and standard deviations (in parentheses) of the overall KL divergence $\text{KL}(f_0(\mathbf{z}), \hat{f}(\mathbf{z}))$ (denoted by $f(\mathbf{z})$), the empirical aggregated KL $1/n \sum_{i=1}^n \text{KL}(f_0(\mathbf{y}|\mathbf{X}_i), \hat{f}(\mathbf{y}|\mathbf{X}_i))$ (denoted by $f(\mathbf{y}|\mathbf{x})$), and $\text{KL}(f_0(\mathbf{x}), \hat{f}(\mathbf{x}))$ (denoted by $f(\mathbf{x})$). cSScGG_CV (cSScGG_LOOKL) and cSScGG_CV_NT (cSScGG_LOOKL_NT) correspond to the cSScGG method without and with normality test respectively, and tuning parameters λ_2 and λ_3 are selected by the 5-fold CV (LOOKL).

Since cSScGG with normality test may identify different \mathbf{X} , we only include the overall KL divergence $\text{KL}(f_0(\mathbf{z}), \hat{f}(\mathbf{z}))$ for comparison. Both versions of the cSScGG method enjoy superior performance relative to all other methods under all settings. When comparing the plain cSScGG with other methods, the differences mainly come from the estimation of $f(\mathbf{x})$, in which parametric methods MLE and QUIC cannot fit the data properly. The cSScGG performs much better than SKDE in both the estimation of $f(\mathbf{x})$ and $f(\mathbf{y}|\mathbf{x})$. When σ is fixed, the performance differences are larger under $\omega = 0.5$ where the deviation from Gaussian is more severe. Furthermore, under a fixed ω , the superiority of

the cSScGG methods is greater when $\sigma = 0.1$ where the deviation from Gaussian is more severe. Comparative results remain the same under other simulation settings (Luo 2018).

5.2 Edge Detection

We do not consider the SKDE and MLE methods here because they do not perform edge selection. In addition to QUIC which is parametric, we also include the nonparanormal (NPN) method (Liu et al. 2009). The NPN method is implemented with the R-package `huge`. When fitting the model, we use shrunken ECDF to transform the data first, then apply Glasso to the transformed data. The final NPN model is selected by the extended BIC score (Foygel & Drton 2010). Given a fixed dimension p , the model chosen by the EBIC method agrees with the model chosen by the BIC method. As the cSScGG method is formulated quite differently from the NPN, our main focus is to investigate the improvements that cSScGG can bring over the QUIC method which assumes normality for all variables including \mathbf{X} .

The performance is measured in three categories: among \mathbf{X} , among \mathbf{Y} , and between \mathbf{X} and \mathbf{Y} . Recall that for the cSScGG procedure, edges in the above categories are decided by Π , Λ and Θ , respectively (see Figure 1). We also report the overall performance based on the whole graph. All simulation results are based on 100 replications.

We fix $p = 25$, $d = 3$, and consider two sample sizes $n = 200$ and $n = 300$. We first generate both \mathbf{X} and \mathbf{Y} from multivariate normals. Specifically, we first generate a $(d + p) \times (d + p)$ sparse precision matrix Ω , in which the probability of the off-diagonal elements being nonzero equals 0.2. Then n i.i.d. samples $\mathbf{Z}_1, \dots, \mathbf{Z}_n$ are generated from $\mathcal{N}(\mathbf{0}, \Omega^{-1})$. The decomposition $\mathbf{Z}_i^T = (\mathbf{X}_i^T, \mathbf{Y}_i^T)$ leads to i.i.d. samples of \mathbf{X} and \mathbf{Y} , and the decomposition $\Omega = \begin{bmatrix} \Omega_{xx} & \Omega_{xy} \\ \Omega_{yx} & \Omega_{yy} \end{bmatrix}$ leads to $\Theta = \Omega_{xy}$ and $\Lambda = \Omega_{yy}$. The results are presented in Table 2.

Overall, the cSScGG and QUIC methods perform better than the NPN. This is expected as the true distribution is Gaussian and the ECDF transformation leads to efficiency loss. Surprisingly, the cSScGG outperforms the QUIC in detecting edges within \mathbf{X} variables even when the normality assumption holds for the QUIC method. It suggests that the proposed projection ratio method

learns the conditional independence within \mathbf{X} better than the parametric QUIC method with BIC. Furthermore, the cSScGG outperforms the QUIC in identifying edges among \mathbf{Y} as well as edges between \mathbf{X} and \mathbf{Y} , due to the fact that there are two penalty parameters in cSScGG, as opposed to one in QUIC. To conclude, the cSScGG method is more efficient even when the joint normality assumption holds.

	cSScGG			QUIC			NPN		
	SPE	SEN	F ₁	SPE	SEN	F ₁	SPE	SEN	F ₁
Among \mathbf{X}									
n=200	0.881	0.931	0.732	0.775	0.97	0.55	0.839	0.914	0.699
	(0.221)	(0.24)	(0.429)	(0.245)	(0.171)	(0.471)	(0.259)	(0.27)	(0.412)
n=300	0.932	0.895	0.827	0.812	0.989	0.713	0.803	0.968	0.765
	(0.203)	(0.278)	(0.352)	(0.293)	(0.102)	(0.428)	(0.304)	(0.17)	(0.372)
Among \mathbf{Y}									
n=200	0.821	0.939	0.707	0.794	0.946	0.682	0.819	0.774	0.564
	(0.029)	(0.039)	(0.035)	(0.03)	(0.037)	(0.034)	(0.095)	(0.333)	(0.197)
n=300	0.858	0.96	0.761	0.829	0.963	0.728	0.79	0.965	0.689
	(0.028)	(0.028)	(0.028)	(0.027)	(0.027)	(0.031)	(0.029)	(0.024)	(0.033)
Between \mathbf{X} and \mathbf{Y}									
n=200	0.828	0.865	0.687	0.776	0.942	0.656	0.821	0.78	0.574
	(0.117)	(0.163)	(0.096)	(0.06)	(0.071)	(0.077)	(0.107)	(0.337)	(0.221)
n=300	0.799	0.966	0.707	0.836	0.969	0.728	0.786	0.955	0.678
	(0.125)	(0.063)	(0.084)	(0.051)	(0.045)	(0.062)	(0.056)	(0.059)	(0.072)
Overall									
n=200	0.823	0.926	0.702	0.79	0.946	0.677	0.82	0.776	0.568
	(0.029)	(0.044)	(0.033)	(0.026)	(0.036)	(0.03)	(0.094)	(0.331)	(0.194)
n=300	0.848	0.96	0.746	0.831	0.964	0.729	0.79	0.963	0.689
	(0.026)	(0.028)	(0.029)	(0.023)	(0.026)	(0.025)	(0.025)	(0.025)	(0.027)

Table 2: Averages and standard deviations (in parentheses) of specificity(SPE), sensitivity(SEN), and F₁ score when $p = 25$ and $d = 3$. \mathbf{X} follows the multivariate Normal distribution.

6 Applications

6.1 Isoprenoid Gene Network in *Arabidopsis Thaliana*

We consider the gene expression data for *Arabidopsis thaliana* introduced by Wille, Zimmermann, Vranová, Fürholz, Laule, Bleuler, Hennig, Prelić, von Rohr & Thiele (2004). *Arabidopsis thaliana* is the first plant to have its genome sequenced, and is a popular model in the study of molecular biology and genetics. The dataset contains $n = 118$ observations of Affymetrix GeneChip microarrays, in which the expression levels of 795 genes are recorded. All values are preprocessed by log-transformation and standardization. This data has been analyzed by Lafferty, Liu & Wasserman (2012) to explore the structure using the nonparanormal model. As in Lafferty et al. (2012), we consider a subset of genes from the isoprenoid pathway ¹.

Our goal is to construct a graph using the proposed cSScGG procedure and compare its structure with those from Glasso (Friedman et al. 2008) and nonparanormal (NPN). Let \mathbf{Z} be the expression levels of 39 genes. To apply the cSScGG procedure we first need to identify variables \mathbf{X} of which the density function may be non-Gaussian. A simple approach is to select elements in \mathbf{Z} whose marginal distributions are non-Gaussian. We looked at histograms of all 39 gene expression levels and found 3 genes (MCT, GGPPS6 and GGPPS1mt) with marginal distribution far from Gaussian, as shown in Figure 2. Therefore, we set \mathbf{X} as gene expression levels of MCT, GGPPS6, and GGPPS1mt. We note that marginal distributions of these three genes have bi-/multiple modes, and monotone transformations cannot transfer them into Gaussian random variables. Therefore, the GGM and nonparanormal model may be inappropriate for this data.

As indicated by Wille et al. (2004), the GGM chosen by the BIC generally leads to a graph that is too dense for biologically relevant researches. Therefore in this study, we construct the graph by limiting the number of edges. Particularly, we tune the regularization parameters in the cSScGG method to fix $|E| = 18$. Results with $|E| = 25$ can be found in Luo (2018). Once the cSScGG fit is obtained, we scan the full regularization path of the Glasso estimates, compare the symmetric difference with the

¹The dataset was downloaded from <https://www.ncbi.nlm.nih.gov/pmc/articles/PMC545783/>. We note that while there were 40 genes in Wille et al. (2004) and Lafferty et al. (2012), this dataset contains 39 only.

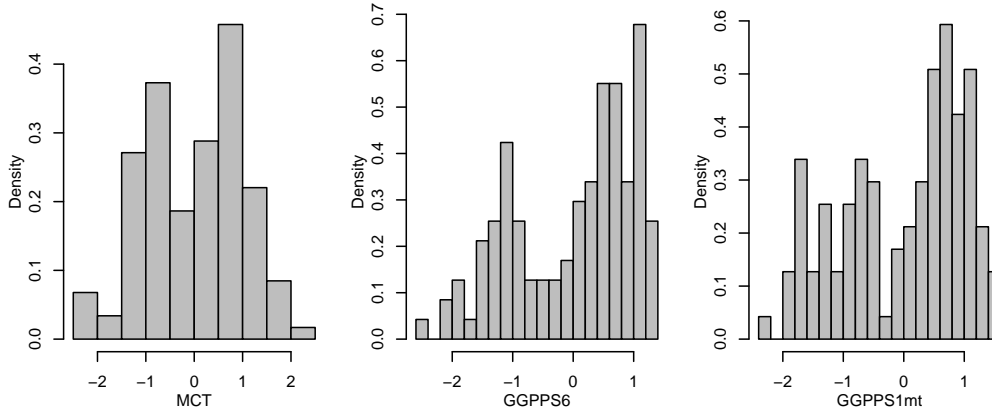


Figure 2: Histogram of three genes in the gene expression data.

cSScGG estimate, and select the graph with smallest symmetric difference value as the Glasso graph. Specifically, the symmetric difference between two graphs is the set of edges which are in either of the graphs but not in their intersection. The same procedure is done for the NPN estimates. We implemented Glasso and NPN with R-packages `glasso` (Friedman, Hastie & Tibshirani 2014) and `huge` (Zhao et al. 2012) respectively.

Figure 3 presents graph topologies achieved from each method, along with the corresponding symmetric difference. We refer the symmetric difference between cSScGG and Glasso to as *cSScGG vs Glasso*, and the symmetric difference between cSScGG and NPN to as *cSScGG vs NPN*. Nodes with numbers 13, 18, and 32 correspond to the 3 non-Gaussian genes GGPPS1mt, GGPPS6, and MCT, respectively. Although the overall structures of different methods look similar, there are some interesting differences.

We focus on the two symmetric difference plots in Figure 3. Note that red edges are selected by the cSScGG only. Most of these edges are associated with the non-Gaussian nodes, for example, edges 32-1 and 32-39. This indicates that the cSScGG procedure is able to discover new interactions for the non-Gaussian variables. We further look at the red lines that appear only in one of the two symmetric difference plots. It is interesting to see that they all come from the *cSScGG vs NPN* plot, indicating that cSScGG is able to detect some edges selected by Glasso which are not selected by NPN. This is not surprising since the cSScGG method assumes a conditional Gaussian distribution for the parametric component. Finally, we note that as a trade-off for the newly identified interactions, there exists

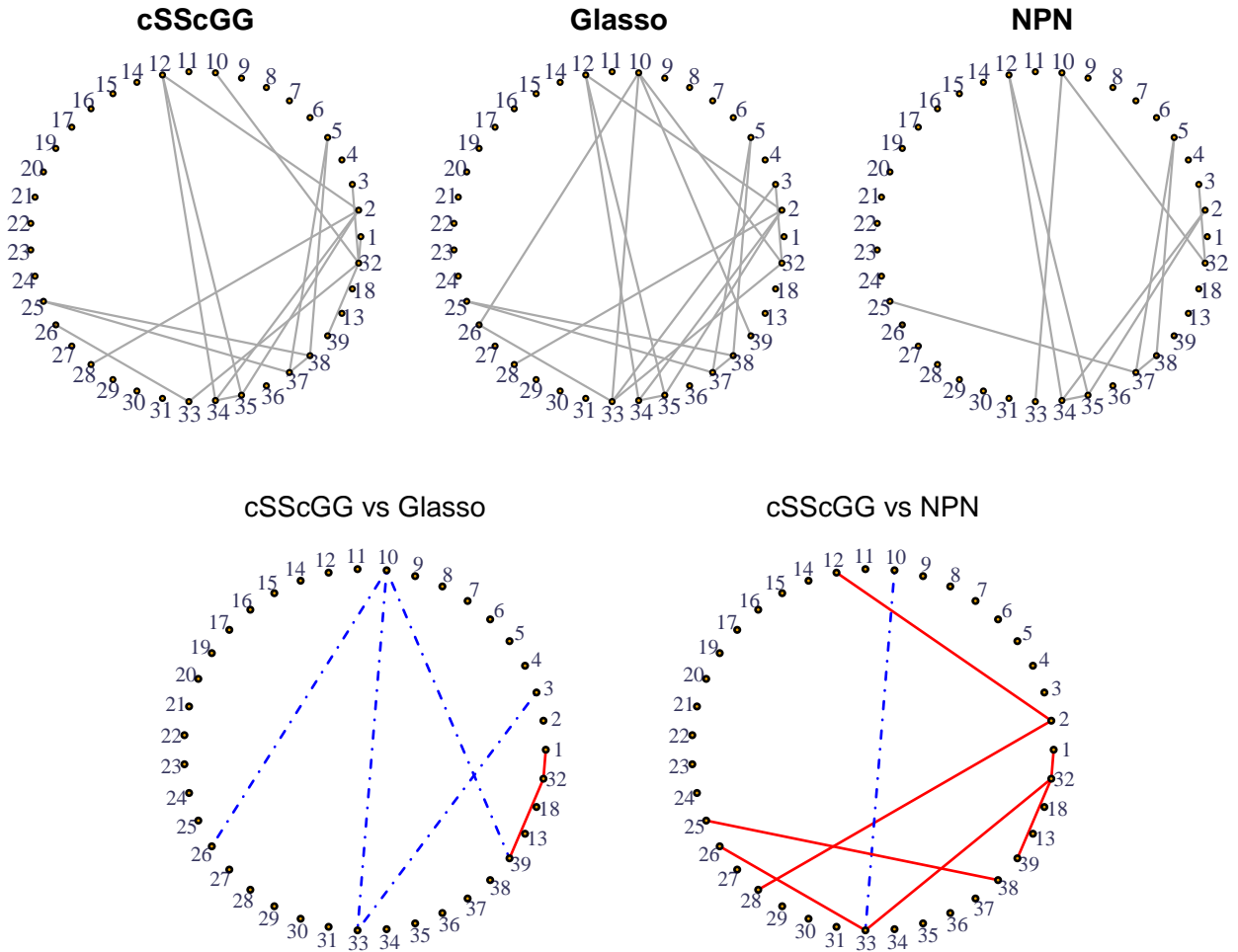


Figure 3: The estimated graph with 18 edges from the cSScGG (*top left*), the closest Glasso (*top middle*), the closest NPN (*top right*), the symmetric difference between cSScGG and Glasso (*bottom left*), and the symmetric difference between cSScGG and NPN (*bottom right*). Red edges — in the bottom represent those selected by the cSScGG but not by the Glasso/NPN, blue edges - - - represent those selected by the Glasso/NPN but not by the cSScGG. Genes GGPPS1mt, GGPPS6, MCT correspond to nodes with numbers 13, 18, 32, respectively.

edges that are selected by both Glasso and NPN, but not by cSScGG. For instance, edge 10-33 with blue dashed line in Figure 3.

To summarize, in terms of the overall graph structure, the cSScGG procedure is capable of capturing a majority of edges that are detected by the Glasso method. By modeling the distributions of some

genes that clearly violate the Gaussian assumption, the proposed method is capable of detecting interactions that are not selected by other methods. These interactions may provide potential research areas for biological study.

6.2 Conditional Relationship Between Clinical, Laboratory and Dialysis Variables from Hemodialysis Patients

We apply the cSScGG procedure to study the conditional relationships between some clinical, laboratory and dialysis variables collected from hemodialysis patients. All patients who underwent dialysis treatments at the Fresenius Medical Care - North America during 2010-2014 are considered. We include patients who stayed at the same facility throughout the treatments. To avoid large fluctuation in the first year on dialysis, we use the average measurements in the second year on dialysis from patients who survived longer than two years. For homogeneity, we include white, non-diabetic and non-Hispanic patients. After removing missing values, we have $n = 2959$ observations (patients) on the following 27 variables in 3 categories:

Clinical variables: `age` (years), `height` (cm), `weight` (kg), `bmi` (body mass index, kg/m^2), `sbp` (systolic blood pressure, mmHg), `dbp` (diastolic blood pressure, mmHg), `temp` (temperature, Celsius);

Laboratory variables: `albumin` (g/dL), `ferritin` (ng/mL), `hgb` (hemoglobin, g/dL), `lymphocytes` (%), `neutrophils` (%), `nlr` (neutrophils to lymphocytes ratio, unitless), `sna` (serum sodium concentration, mEq/L or mmol/L), `wbc` (white blood cell, 1000/mc);

Dialysis variables: `qb` (blood flow, mL/min), `qd` (dialysis flow, mL/min), `saline` (mL), `txttime` (treatment time, min), `olc` (on-line clearance, unitless), `idwg` (interdialytic weight gain, kg), `ufv` (ultrafiltration volume, L), `ufr` (ultrafiltration rate, mL/hr/kg), `epodose` (erythropoietin dose, unit), `volume` (L), `enpcr` (equilibrated normalized protein catabolic rate, g/kg/day), `ektv` (equilibrated Kt/V , unitless).

Note that `nlr` and `epodose` have been transformed to make them close to Gaussian. In particular, `nlr` equals the logarithm of the neutrophils to lymphocytes ratio, and `epodose` represents the $1/4$ power transformation of the actual erythropoietin dose.

The primary objective of this study is to discover the interactions between all these measurements.

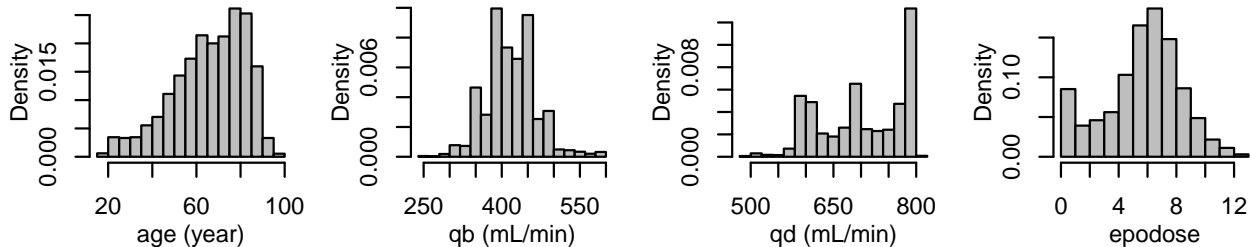


Figure 4: Histograms of age, qb, qd and epodose.

We first check the marginal distributions of all 27 variables to investigate possible violation of the Gaussian assumption. We identify 4 variables, `age`, `qb`, `qd` and `epodose` as non-Gaussian with very small p-values (less than 2×10^{-16}). Histograms in Figure 4 indicate that the distribution of `age` is skewed, and the distributions of `qb`, `qd` and `epodose` have multiple peaks. Note that despite the 1/4 power transformation, the distribution of `epodose` is still far from normal due to the point mass at zero. Consequently, we specify these 4 variables as \mathbf{X} to be estimated nonparametrically in the proposed cSScGG procedure.

We compare the cSScGG procedure with Glasso and NPN. For the NPN method, we use the shrunken ECDF to transform the data first, then apply Glasso to the transformed data. For each method, we tune the regularization parameters by BIC. The estimated graph structures are shown in Figure 5.

From the visual inspection, there is a large set of edges shared by cSScGG and Glasso, which is due to the fact that cSScGG assumes majority of the variables are conditionally normal. However, the graph of Glasso is much denser. To see how cSScGG differs from other two methods, Figure 6 shows edges detected by the cSScGG procedure only. It shows that the `bmi` is a hub node whose connections with other variables such as `age`, `dbp`, and `wbc` are not selected by other methods. Meanwhile, `qb` has multiple connections with nodes from the other two categories (Clinical and Laboratory). The value of these extra edges remains to be further explored from a clinical standpoint. We do not intend to claim that the graph obtained by the cSScGG procedure is the best as the underlying truth is unknown. Instead, with different model assumptions, the cSScGG procedure can identify potential links for further study.

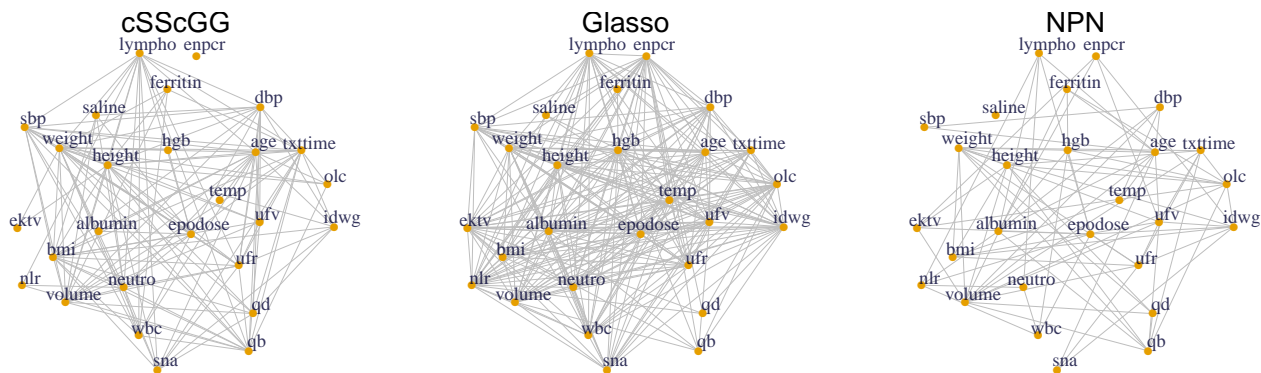


Figure 5: The estimated graphs using cSScGG (*left*), Glasso (*middle*), and NPN (*right*). Tuning parameters are selected by the BIC method. Layout of nodes are fixed across four topologies.

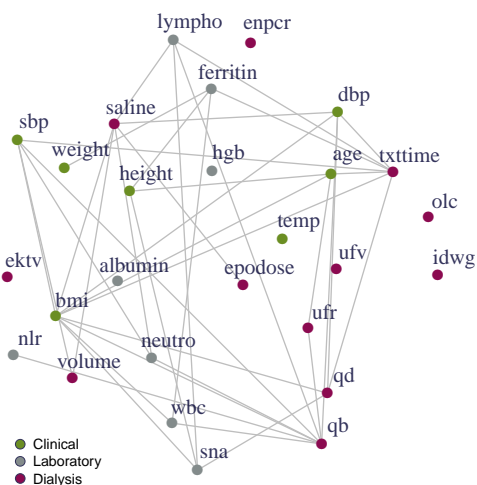


Figure 6: Edges exclusively detected by cSScGG. The measurements are grouped into three categories as described at beginning of Section 6.2.

References

- Allen, G. I. and Liu, Z. (2012). A log-linear graphical model for inferring genetic networks from high-throughput sequencing data, *Bioinformatics and Biomedicine (BIBM), 2012 IEEE International Conference on*, IEEE, pp. 1–6.
- Armijo, L. (1966). Minimization of functions having Lipschitz continuous first partial derivatives, *Pacific Journal of Mathematics* **16**: 1–3.

- Duong, T. (2007). ks: Kernel density estimation and kernel discriminant analysis for multivariate data in R, *Journal of Statistical Software* **21**: 1–16.
- Fan, J. and Li, R. (2001). Variable selection via nonconcave penalized likelihood and its oracle properties, *Journal of the American Statistical Association* **96**: 1348–1360.
- Fan, J., Liao, Y. and Liu, H. (2016). An overview of the estimation of large covariance and precision matrices, *The Econometrics Journal* **19**: C1–C32.
- Fan, J., Liao, Y. and Mincheva, M. (2011). High dimensional covariance matrix estimation in approximate factor models, *Annals of Statistics* **39**: 3320–3356.
- Fellinghauer, B., Bühlmann, P., Ryffel, M., Von Rhein, M. and Reinhardt, J. D. (2013). Stable graphical model estimation with random forests for discrete, continuous, and mixed variables, *Computational Statistics & Data Analysis* **64**: 132–152.
- Finegold, M. and Drton, M. (2011). Robust graphical modeling of gene networks using classical and alternative t-distributions, *The Annals of Applied Statistics* **5**: 1057–1080.
- Foygel, R. and Drton, M. (2010). Extended Bayesian information criteria for Gaussian graphical models, *Advances in Neural Information Processing Systems*, pp. 2020–2028.
- Friedman, J. H., Stuetzle, W. and Schroeder, A. (1984). Projection pursuit density estimation, *Journal of the American Statistical Association* **79**: 599–608.
- Friedman, J., Hastie, T. and Tibshirani, R. (2008). Sparse inverse covariance estimation with the graphical lasso, *Biostatistics* **9**: 432–441.
- Friedman, J., Hastie, T. and Tibshirani, R. (2014). Glasso: graphical lasso-estimation of gaussian graphical models. r package version 1.8.
- Genest, C., Ghoudi, K. and Rivest, L. (1995). A semiparametric estimation procedure of dependence parameters in multivariate families of distribution, *Biometrika* **82**: 543–552.
- Gu, C. (2013). *Smoothing Spline ANOVA Models*, Vol. 297, Springer Science & Business Media.

- Gu, C. (2014). Smoothing spline ANOVA models: R package *gss*, *Journal of Statistical Software* **58**: 1–25.
- Gu, C., Jeon, Y. and Lin, Y. (2013). Nonparametric density estimation in high-dimensions, *Statistica Sinica* **23**: 1131–1153.
- Höfling, H. and Tibshirani, R. (2009). Estimation of sparse binary pairwise markov networks using pseudo-likelihoods, *Journal of Machine Learning Research* **10**: 883–906.
- Hoti, F. and Holmström, L. (2004). A semiparametric density estimation approach to pattern classification, *Pattern Recognition* **37**: 409–419.
- Hsieh, C.-J., Dhillon, I. S., Ravikumar, P. K. and Sustik, M. A. (2011). Sparse inverse covariance matrix estimation using quadratic approximation, *Advances in Neural Information Processing Systems*, pp. 2330–2338.
- Hsieh, C.-J., Sustik, M. A., Dhillon, I. S. and Ravikumar, P. (2014). QUIC: quadratic approximation for sparse inverse covariance estimation, *The Journal of Machine Learning Research* **15**: 2911–2947.
- Jeon, Y. and Lin, Y. (2006). An effective method for high-dimensional log-density ANOVA estimation, with application to nonparametric graphical model building, *Statistica Sinica* **16**: 353–374.
- Kendall, M., Stuart, A. and Ord, J. (1987). *Kendall’s Advanced Theory of Statistics*, Oxford University Press.
- Lafferty, J., Liu, H. and Wasserman, L. (2012). Sparse nonparametric graphical models, *Statistical Science* **27**: 519–537.
- Lauritzen, S. L. (1996). *Graphical Models*, Vol. 17, Clarendon Press.
- Lee, S.-I., Ganapathi, V. and Koller, D. (2007). Efficient structure learning of markov networks using l_1 -regularization, *Advances in Neural Information Processing Systems*, pp. 817–824.

- Lee, W. and Liu, Y. (2012). Simultaneous multiple response regression and inverse covariance matrix estimation via penalized Gaussian maximum likelihood, *Journal of Multivariate Analysis* **111**: 241–255.
- Li, D., Yang, K. and Wong, W. H. (2016). Density estimation via discrepancy based adaptive sequential partition, *Advances in Neural Information Processing Systems*, pp. 1091–1099.
- Lian, H. (2011). Shrinkage tuning parameter selection in precision matrices estimation, *Journal of Statistical Planning and Inference* **141**: 2839–2848.
- Lin, L. (2018). *Methods for Estimation and Inference for High-Dimensional Models*, PhD thesis, University of Washington.
- Liu, H., Han, F., Yuan, M., Lafferty, J. and Wasserman, L. (2012). High-dimensional semiparametric Gaussian copula graphical models, *The Annals of Statistics* **40**: 2293–2326.
- Liu, H., Lafferty, J. and Wasserman, L. (2007). Sparse nonparametric density estimation in high dimensions using the rodeo, *Artificial Intelligence and Statistics*, pp. 283–290.
- Liu, H., Lafferty, J. and Wasserman, L. (2009). The nonparanormal: Semiparametric estimation of high dimensional undirected graphs, *Journal of Machine Learning Research* **10**: 2295–2328.
- Liu, H., Xu, M., Gu, H., Gupta, A., Lafferty, J. and Wasserman, L. (2011). Forest density estimation, *Journal of Machine Learning Research* **12**: 907–951.
- Liu, L. and Wong, W. H. (2014). *Multivariate density estimation based on adaptive partitioning: Convergence rate, variable selection and spatial adaptation*, Department of Statistics, Stanford University.
- Loader, C. R. (1996). Local likelihood density estimation, *The Annals of Statistics* **24**: 1602–1618.
- Lu, L., Jiang, H. and Wong, W. H. (2013). Multivariate density estimation by Bayesian sequential partitioning, *Journal of the American Statistical Association* **108**: 1402–1410.
- Luo, R. (2018). *Multivariate Density Estimation and Graphical Models*, PhD thesis, University of California - Santa Barbara.

- McCarter, C. and Kim, S. (2016). Large-scale optimization algorithms for sparse conditional Gaussian graphical models, *Artificial Intelligence and Statistics*, pp. 528–537.
- Miyamura, M. and Kano, Y. (2006). Robust Gaussian graphical modeling, *Journal of Multivariate Analysis* **97**: 1525–1550.
- Oh, J. H. (2017). *Graphical Models for non-Gaussian Continuous Data with Applications to Genomics Datasets*, PhD thesis, Purdue University.
- Parzen, E. (1962). On estimation of a probability density function and mode, *The Annals of Mathematical Statistics* **33**: 1065–1076.
- Ram, P. and Gray, A. (2011). Density estimation trees, *Proceedings of the 17th ACM SIGKDD International Conference on Knowledge Discovery and Data Mining*, pp. 627–635.
- Ravikumar, P., Wainwright, M. J. and Lafferty, J. D. (2010). High-dimensional Ising model selection using ℓ_1 -regularized logistic regression, *The Annals of Statistics* **38**: 1287–1319.
- Ravikumar, P., Wainwright, M. J., Raskutti, G. and Yu, B. (2011). High-dimensional covariance estimation by minimizing ℓ_1 -penalized log-determinant divergence, *Electronic Journal of Statistics* **5**: 935–980.
- Richardson, S. and Green, P. J. (1997). On Bayesian analysis of mixtures with an unknown number of components (with discussion), *Journal of the Royal Statistical Society: Series B (Statistical Methodology)* **59**: 731–792.
- Silverman, B. W. (2018). *Density Estimation for Statistics and Data Analysis*, Routledge.
- Sohn, K.-A. and Kim, S. (2012). Joint estimation of structured sparsity and output structure in multiple-output regression via inverse-covariance regularization, *Artificial Intelligence and Statistics*, pp. 1081–1089.
- Sun, H. and Li, H. (2012). Robust Gaussian graphical modeling via ℓ_1 penalization, *Biometrics* **68**: 1197–1206.

- Vogel, D. and Fried, R. (2011). Elliptical graphical modelling, *Biometrika* **98**: 935–951.
- Vujačić, I., Abbruzzo, A. and Wit, E. (2015). A computationally fast alternative to cross-validation in penalized Gaussian graphical models, *Journal of Statistical Computation and Simulation* **85**: 3628–3640.
- Wainwright, M. J. (2009). Sharp thresholds for high-dimensional and noisy sparsity recovery using ℓ_1 -constrained quadratic programming (lasso), *IEEE Transactions on Information Theory* **55**: 2183–2202.
- Wang, Y. (2011). *Smoothing Splines: Methods and Applications*, Chapman and Hall/CRC.
- Wang, Y., Canale, A. and Dunson, D. (2016). Scalable geometric density estimation, *Proceedings of the 19th International Conference on Artificial Intelligence and Statistics (AISTATS)*, pp. 857–865.
- Wille, A., Zimmermann, P., Vranová, E., Fürholz, A., Laule, O., Bleuler, S., Hennig, L., Prelić, A., von Rohr, P. and Thiele, L. (2004). Sparse graphical Bayesian modeling of the isoprenoid gene network in *Arabidopsis thaliana*, *Genome Biology* **5**: R92.
- Wytock, M. and Kolter, Z. (2013). Sparse Gaussian conditional random fields: Algorithms, theory, and application to energy forecasting, *International Conference on Machine Learning*, pp. 1265–1273.
- Xue, L. and Zou, H. (2012). Regularized rank-based estimation of high-dimensional nonparanormal graphical models, *The Annals of Statistics* **40**: 2541–2571.
- Yanagihara, H., Tonda, T. and Matsumoto, C. (2006). Bias correction of cross-validation criterion based on Kullback–Leibler information under a general condition, *Journal of Multivariate Analysis* **97**: 1965–1975.
- Yang, E., Allen, G., Liu, Z. and Ravikumar, P. K. (2012). Graphical models via generalized linear models, *Advances in Neural Information Processing Systems*, pp. 1358–1366.
- Yin, J. and Li, H. (2011). A sparse conditional Gaussian graphical model for analysis of genetical genomics data, *The Annals of Applied Statistics* **5**: 2630.

Yuan, X.-T. and Zhang, T. (2014). Partial Gaussian graphical model estimation, *IEEE Transactions on Information Theory* **60**: 1673–1687.

Zhao, T., Liu, H., Roeder, K., Lafferty, J. and Wasserman, L. (2012). The huge package for high-dimensional undirected graph estimation in R, *Journal of Machine Learning Research* **13**: 1059–1062.

Zou, H. (2006). The adaptive lasso and its oracle properties, *Journal of the American Statistical Association* **101**: 1418–1429.

Appendix A Derivation of the LOOKL

Our derivation is similar to that in Lian (2011) and Vujačić et al. (2015) with adjustments to deal with complications brought by the conditional mean $-\Lambda^{-1}\Theta^T\mathbf{x}$ and two tuning parameters. Recall that a cGGM assumes that $\mathbf{Y}|\mathbf{X} = \mathbf{x} \sim \mathcal{N}(-\Lambda^{-1}\Theta^T\mathbf{x}, \Lambda^{-1})$. The log-likelihood based on the k -th observation \mathbf{X}_k and \mathbf{Y}_k is (ignoring constant terms)

$$\tilde{l}_k(\Lambda, \Theta) = \frac{1}{2} \{ \log |\Lambda| - \text{tr}(S_{yy,k}\Lambda + 2S_{xy,k}^T\Theta + \Lambda^{-1}\Theta^T S_{xx,k}^T\Theta) \}, \quad (\text{A.1})$$

where $S_{yy,k} = \mathbf{Y}_k^T\mathbf{Y}_k$, $S_{xy,k} = \mathbf{X}_k^T\mathbf{Y}_k$, and $S_{xx,k} = \mathbf{X}_k^T\mathbf{X}_k$ are the empirical variance/covariance matrices. Note that $S_{yy} = n^{-1} \sum_{k=1}^n S_{yy,k}$, $S_{xx} = n^{-1} \sum_{k=1}^n S_{xx,k}$, and $S_{xy} = n^{-1} \sum_{k=1}^n S_{xy,k}$.

Let $\hat{\Lambda}^{(-k)}$ and $\hat{\Theta}^{(-k)}$ be the estimates of Λ and Θ based on the data excluding the k -th observation. Directly calculating leave-one-out estimate of the KL distance is computationally costly. We now derive a score based on the fact that cross-validating the log-likelihood provides an estimate of the KL distance (Yanagihara, Tonda and Matsumoto, 2006).

Consider the following function of five variables $f(S_{xx}, S_{yy}, S_{xy}, \Lambda, \Theta) = \log |\Lambda| - \text{tr}(S_{yy}\Lambda + 2S_{xy}^T\Theta + \Lambda^{-1}\Theta^T S_{xx}^T\Theta)$. We have the identity $\sum_{k=1}^n f(S_{xx,k}, S_{yy,k}, S_{xy,k}, \Lambda, \Theta) = nf(S_{xx}, S_{yy}, S_{xy}, \Lambda, \Theta)$. Letting $\mathbf{S} = (S_{xx}, S_{yy}, S_{xy})$ and $\mathbf{S}_k = (S_{xx,k}, S_{yy,k}, S_{xy,k})$, we denote $f(S_{xx}, S_{yy}, S_{xy}, \Lambda, \Theta)$ and $f(S_{xx,k}, S_{yy,k}, S_{xy,k}, \Lambda, \Theta)$ as $f(\mathbf{S}, \Lambda, \Theta)$ and $f(\mathbf{S}_k, \Lambda, \Theta)$ in the rest of the derivation. The leave-one-out

cross validation score (Yanagihara et al., 2006)

$$\begin{aligned}
\text{LOOCV} &= -\frac{1}{n} \sum_{k=1}^n \tilde{l}_k(\hat{\Lambda}^{(-k)}, \hat{\Theta}^{(-k)}) = -\frac{1}{2n} \sum_{k=1}^n f(\mathbf{S}_k, \hat{\Lambda}^{(-k)}, \hat{\Theta}^{(-k)}) \\
&= -\frac{1}{2} f(\mathbf{S}, \hat{\Lambda}, \hat{\Theta}) - \frac{1}{2n} \sum_{k=1}^n \{f(\mathbf{S}_k, \hat{\Lambda}^{(-k)}, \hat{\Theta}^{(-k)}) - f(\mathbf{S}_k, \hat{\Lambda}, \hat{\Theta})\} \\
&\approx -\frac{1}{n} l_2(\hat{\Lambda}, \hat{\Theta}) - \frac{1}{2n} \sum_{k=1}^n \left\{ \left(\frac{\partial f(\mathbf{S}_k, \hat{\Lambda}, \hat{\Theta})}{\partial \Lambda} \right)^T \text{vec}(\hat{\Lambda}^{(-k)} - \hat{\Lambda}) + \left(\frac{\partial f(\mathbf{S}_k, \hat{\Lambda}, \hat{\Theta})}{\partial \Theta} \right)^T \text{vec}(\hat{\Theta}^{(-k)} - \hat{\Theta}) \right\},
\end{aligned} \tag{A.2}$$

where $\partial f(\mathbf{S}_k, \hat{\Lambda}, \hat{\Theta})/\partial \Lambda = \partial f(\mathbf{S}_k, \hat{\Lambda}, \hat{\Theta})/\partial \text{vec}(\Lambda)$ and $\partial f(\mathbf{S}_k, \hat{\Lambda}, \hat{\Theta})/\partial \Theta = \partial f(\mathbf{S}_k, \hat{\Lambda}, \hat{\Theta})/\partial \text{vec}(\Theta)$ are p^2 and pd dimensional column vectors of partial derivatives given by

$$\mathbf{u}_k \triangleq \frac{\partial f(\mathbf{S}_k, \hat{\Lambda}, \hat{\Theta})}{\partial \Lambda} = \text{vec}(\Lambda^{-1} - S_{yy,k} + \Lambda^{-1} \hat{\Theta}^T S_{xx,k} \hat{\Theta} \Lambda^{-1}), \tag{A.3}$$

$$\mathbf{w}_k \triangleq \frac{\partial f(\mathbf{S}_k, \hat{\Lambda}, \hat{\Theta})}{\partial \Theta} = \text{vec}(-2S_{xy,k} - 2S_{xx,k} \Theta \hat{\Lambda}^{-1}). \tag{A.4}$$

Denoting $\mathbf{S}^{(-k)}$ as the version of \mathbf{S} without the k -th observation, the Taylor expansions of the functions $\partial f(\mathbf{S}^{(-k)}, \hat{\Lambda}^{(-k)}, \hat{\Theta}^{(-k)})/\partial \Lambda$ and $\partial f(\mathbf{S}^{(-k)}, \hat{\Lambda}^{(-k)}, \hat{\Theta}^{(-k)})/\partial \Theta$ at the point $(\mathbf{S}, \hat{\Lambda}, \hat{\Theta})$ are

$$\begin{aligned}
\mathbf{0}_{p^2} &= \frac{\partial f(\mathbf{S}^{(-k)}, \hat{\Lambda}^{(-k)}, \hat{\Theta}^{(-k)})}{\partial \Lambda} \\
&\approx \frac{\partial f(\mathbf{S}, \hat{\Lambda}, \hat{\Theta})}{\partial \Lambda} + \frac{\partial^2 f(\mathbf{S}, \hat{\Lambda}, \hat{\Theta})}{\partial \Lambda^2} \text{vec}(\hat{\Lambda}^{(-k)} - \hat{\Lambda}) + \frac{\partial^2 f(\mathbf{S}, \hat{\Lambda}, \hat{\Theta})}{\partial \Lambda \partial \Theta} \text{vec}(\hat{\Theta}^{(-k)} - \hat{\Theta}) \\
&\quad + \frac{\partial^2 f(\mathbf{S}, \hat{\Lambda}, \hat{\Theta})}{\partial \Lambda \partial S_{xx}} \text{vec}(S_{xx}^{(-k)} - S_{xx}) + \frac{\partial^2 f(\mathbf{S}, \hat{\Lambda}, \hat{\Theta})}{\partial \Lambda \partial S_{yy}} \text{vec}(S_{yy}^{(-k)} - S_{yy}) \\
&\quad + \frac{\partial^2 f(\mathbf{S}, \hat{\Lambda}, \hat{\Theta})}{\partial \Lambda \partial S_{xy}} \text{vec}(S_{xy}^{(-k)} - S_{xy}),
\end{aligned} \tag{A.5}$$

and

$$\begin{aligned}
\mathbf{0}_{pd} &= \frac{\partial f(\mathbf{S}^{(-k)}, \hat{\Lambda}^{(-k)}, \hat{\Theta}^{(-k)})}{\partial \Theta} \\
&\approx \frac{\partial f(\mathbf{S}, \hat{\Lambda}, \hat{\Theta})}{\partial \Theta} + \frac{\partial^2 f(\mathbf{S}, \hat{\Lambda}, \hat{\Theta})}{\partial \Theta^2} \text{vec}(\hat{\Theta}^{(-k)} - \hat{\Theta}) + \frac{\partial^2 f(\mathbf{S}, \hat{\Lambda}, \hat{\Theta})}{\partial \Theta \partial \Lambda} \text{vec}(\hat{\Lambda}^{(-k)} - \hat{\Lambda}) \\
&\quad + \frac{\partial^2 f(\mathbf{S}, \hat{\Lambda}, \hat{\Theta})}{\partial \Theta \partial S_{xx}} \text{vec}(S_{xx}^{(-k)} - S_{xx}) + \frac{\partial^2 f(\mathbf{S}, \hat{\Lambda}, \hat{\Theta})}{\partial \Theta \partial S_{xy}} \text{vec}(S_{xy}^{(-k)} - S_{xy}) \\
&\quad + \frac{\partial^2 f(\mathbf{S}, \hat{\Lambda}, \hat{\Theta})}{\partial \Theta \partial S_{yy}} \text{vec}(S_{yy}^{(-k)} - S_{yy}),
\end{aligned} \tag{A.6}$$

where $\partial^2 f(\mathbf{S}, \Lambda, \Theta)/\partial \Lambda^2 = (\partial f(\mathbf{S}, \Lambda, \Theta)/\partial \text{vec}(\Lambda))/\partial \text{vec}(\Lambda)$ is the $p^2 \times p^2$ Hessian matrix, $\partial f(\mathbf{S}, \hat{\Lambda}, \hat{\Theta})/\partial \Lambda$ and $\partial f(\mathbf{S}, \hat{\Lambda}, \hat{\Theta})/\partial \Theta$ denote partial derivative evaluated at $\hat{\Lambda}$ and $\hat{\Theta}$, and other second order derivatives are defined similarly. Note that $\partial f(\mathbf{S}, \hat{\Lambda}, \hat{\Theta})/\partial \Lambda = \mathbf{0}$ and $\partial f(\mathbf{S}, \hat{\Lambda}, \hat{\Theta})/\partial \Theta = \mathbf{0}$ because $\hat{\Lambda}$

and $\hat{\Theta}$ are the maximum likelihood estimators, $\partial^2 f(\mathbf{S}, \hat{\Lambda}, \hat{\Theta})/\partial\Lambda\partial S_{xy} = \mathbf{0}$ because (A.3) is free of S_{xy} , and $\partial^2 f(\mathbf{S}, \hat{\Lambda}, \hat{\Theta})/\partial\Theta\partial S_{yy} = \mathbf{0}$ because (A.4) is free of S_{yy} . Let $A = \partial^2 f(\mathbf{S}, \hat{\Lambda}, \hat{\Theta})/\partial\Theta^2 = -2\hat{\Lambda}^{-1} \otimes S_{xx}$, $B = \partial^2 f(\mathbf{S}, \hat{\Lambda}, \hat{\Theta})/\partial\Theta\partial\Lambda = 2\hat{\Lambda}^{-1} \otimes S_{xx} \hat{\Theta} \hat{\Lambda}^{-1}$, $C = \partial^2 f(\mathbf{S}, \hat{\Lambda}, \hat{\Theta})/\partial\Lambda^2 = -\hat{\Lambda}^{-1} \otimes (\hat{\Lambda}^{-1} + 2\hat{\Lambda}^{-1} \hat{\Theta}^T S_{xx} \hat{\Theta} \hat{\Lambda}^{-1})$, $D = \partial^2 f(\mathbf{S}, \hat{\Lambda}, \hat{\Theta})/\partial\Theta\partial S_{xx} = -2\hat{\Lambda}^{-1} \hat{\Theta}^T \otimes I_{d \times d}$, and $E = \partial^2 f(\mathbf{S}, \hat{\Lambda}, \hat{\Theta})/\partial\Lambda\partial S_{xx} = \hat{\Lambda}^{-1} \hat{\Theta}^T \otimes \hat{\Lambda}^{-1} \hat{\Theta}^T$. Solving (A.5) and (A.6) and plugging solutions into (A.2), we have

$$\begin{aligned} & \text{LOOKL}(\lambda_2, \lambda_3) \\ &= -\frac{1}{n} l_2(\hat{\Lambda}, \hat{\Theta}) + \frac{1}{2n} \sum_{k=1}^n \left\{ \mathbf{u}_k^T (-C + B^T A^{-1} B)^{-1} [(-E + B^T A^{-1} D) \mathbf{v}_{xx,k} + 2B^T A^{-1} \mathbf{v}_{xy,k} - \mathbf{v}_{yy,k}] \right. \\ & \quad \left. + \mathbf{w}_k^T (-A + BC^{-1} B^T)^{-1} [(D - BC^{-1} E) \mathbf{v}_{xx,k} + BC^{-1} \mathbf{v}_{yy,k} - 2\mathbf{v}_{xy,k}] \right\}. \end{aligned} \quad (\text{A.7})$$

For the Gaussian graphical model with $\mathbf{Y} \sim \mathcal{N}(\mathbf{0}, \Lambda^{-1})$, (A.7) reduces to

$$-\frac{1}{n} l_2(\hat{\Lambda}) + \frac{1}{2n} \sum_{k=1}^n \text{vec}(\Lambda^{-1} - S_{yy,k})^T (\hat{\Lambda} \otimes \hat{\Lambda}) \text{vec}(S_{yy}^{(-k)} - S_{yy}),$$

which is the same as the GACV in Lian (2011) and KLCV in Vujačić et al. (2015).

Appendix B Calculation of the Projection Ratio

Letting $\hat{\zeta}(\mathbf{x}) = \hat{\Delta}(\mathbf{x}) + \hat{\eta}(\mathbf{x})$, we construct the ratio $\tilde{V}(\hat{\zeta} - \tilde{\zeta})/\tilde{V}(\hat{\zeta} - \eta_u)$ where $\tilde{\zeta}$ denotes the squared error projection of $\hat{\zeta}$ in \mathcal{S}^0 . A small ratio indicates that \mathcal{S}^1 may be removed. By definition,

$$\begin{aligned} \tilde{V}(\hat{\zeta} - \eta_u) &= \int_{\mathcal{X}} (\hat{\eta} + \hat{\Delta} - \eta_u)^2 \rho(\mathbf{x}) d\mathbf{x} - \left\{ \int_{\mathcal{X}} (\hat{\eta} + \hat{\Delta} - \eta_u) \rho(\mathbf{x}) d\mathbf{x} \right\}^2 \\ &\triangleq \tilde{V}(\hat{\eta} - \eta_u) + \tilde{V}(\hat{\Delta}, \hat{\Delta}) + 2\tilde{V}(\hat{\eta} - \eta_u, \hat{\Delta}). \end{aligned} \quad (\text{A.8})$$

To obtain $\tilde{V}(\hat{\zeta} - \tilde{\zeta})$, one needs to find

$$\tilde{\zeta} = \arg \min_{\zeta = \hat{\eta} + \hat{\Delta}, \eta \in \mathcal{S}^0} \left\{ \int_{\mathcal{X}} (\hat{\eta} + \hat{\Delta} - \eta)^2(\mathbf{x}) \rho(\mathbf{x}) d\mathbf{x} - \left\{ \int_{\mathcal{X}} (\hat{\eta} + \hat{\Delta} - \eta)(\mathbf{x}) \rho(\mathbf{x}) d\mathbf{x} \right\}^2 \right\}. \quad (\text{A.9})$$

Let $\mathcal{S}^0 = \mathcal{H}^0 \oplus \mathcal{H}^1$, where \mathcal{H}^0 is a space spanned by known functions $\{\varphi_1(\mathbf{x}), \dots, \varphi_m(\mathbf{x})\}$ and \mathcal{H}^1 is the orthogonal reproducing kernel Hilbert space with the reproducing kernel function $R(\cdot, \cdot)$. Let $\boldsymbol{\phi} = (\varphi_i(\mathbf{X}_j))_{i=1, \dots, m}^{j=1, \dots, n}$ and $\boldsymbol{\xi} = (R(\mathbf{X}_i, \mathbf{X}_j))_{i=1, \dots, n}^{j=1, \dots, n}$. Let $\tilde{\zeta} = \boldsymbol{\phi}^T \tilde{\mathbf{d}} + \boldsymbol{\xi}^T \tilde{\mathbf{c}}$, take derivatives with respect

to $\tilde{\mathbf{d}}$ and $\tilde{\mathbf{c}}$, and set them to zero. After rearrangements, we obtain the equation

$$\begin{bmatrix} \tilde{V}(\boldsymbol{\phi}, \boldsymbol{\phi}) & \tilde{V}(\boldsymbol{\phi}, \boldsymbol{\xi}) \\ \tilde{V}(\boldsymbol{\xi}, \boldsymbol{\phi}) & \tilde{V}(\boldsymbol{\xi}, \boldsymbol{\xi}) \end{bmatrix} \begin{bmatrix} \tilde{\mathbf{d}} \\ \tilde{\mathbf{c}} \end{bmatrix} = \begin{bmatrix} \tilde{V}(\hat{\boldsymbol{\eta}} + \hat{\Delta}, \boldsymbol{\phi}) \\ \tilde{V}(\hat{\boldsymbol{\eta}} + \hat{\Delta}, \boldsymbol{\xi}) \end{bmatrix}, \quad (\text{A.10})$$

where $\tilde{V}(\mathbf{a}, \mathbf{b}) = \{\tilde{V}(a_i, b_j)\}_{i=1}^I \{\}_{j=1}^J$ for any vectors of functions $\mathbf{a} = (a_1, \dots, a_I)^T$ and $\mathbf{b} = (b_1, \dots, b_J)^T$.

The right hand side of (A.10) contains some extra components involving $\hat{\Delta}$. We compute solutions to (A.10) using the Cholesky decomposition implemented in the `project()` function in the R package `gss` (Gu, 2014). Once $\tilde{\boldsymbol{\zeta}}$ is computed, we have

$$\tilde{V}(\hat{\boldsymbol{\zeta}} - \tilde{\boldsymbol{\zeta}}) = \int_{\mathcal{X}} (\hat{\boldsymbol{\zeta}} - \tilde{\boldsymbol{\zeta}})^2(\mathbf{x}) \rho(\mathbf{x}) d\mathbf{x} - \left\{ \int_{\mathcal{X}} (\hat{\boldsymbol{\zeta}} - \tilde{\boldsymbol{\zeta}})(\mathbf{x}) \rho(\mathbf{x}) d\mathbf{x} \right\}^2 = \tilde{V}(\hat{\boldsymbol{\zeta}}, \hat{\boldsymbol{\zeta}}) + \tilde{V}(\tilde{\boldsymbol{\zeta}}, \tilde{\boldsymbol{\zeta}}) - 2\tilde{V}(\tilde{\boldsymbol{\zeta}}, \hat{\boldsymbol{\zeta}}). \quad (\text{A.11})$$

Appendix C Proofs of Theoretical Results

To prove Theorem 1, we first introduce a sequence of lemmas as in Wytock and Koltner (2013). Note that, different from Wytock and Koltner (2013), we allow different penalties for Λ and Θ . Lemma 1 below studies the decay rate of the gradients $\nabla_{\Theta} l_2(\Lambda_0, \Theta_0)$ and $\nabla_{\Lambda} l_2(\Lambda_0, \Theta_0)$ in element-wise infinity operator norm as sample size increases.

Lemma 1. *Suppose that the Assumption 1 holds. Then*

$$\mathbb{P}(\|\nabla_{\Theta} l_2(\Lambda_0, \Theta_0)\|_{\infty} > \vartheta) \leq 2dp \exp \left\{ -\frac{n\vartheta^2}{8C_{\sigma}^2 C_X^2} \right\}, \quad (\text{A.12})$$

$$\mathbb{P}(\|\nabla_{\Lambda} l_2(\Lambda_0, \Theta_0)\|_{\infty} > \vartheta) \leq 4p^2 \exp \left\{ -\frac{n\vartheta^2}{3200C_{\sigma}^2} \right\}, \quad (\text{A.13})$$

for any $\vartheta \in (0, 40C_{\sigma})$.

Proof. Wytock and Koltner (2013) proved (A.12) using the Chernoff bound for the Gaussian tail probability. Ravikumar, Wainwright, Raskutti and Yu (2011) proved (A.13) in their Lemma 1. \square

The next lemma extends the primal-dual witness approach proposed in Wainwright (2009) to our multi-penalties setting. Let $\Gamma = (\Lambda^T, \Theta^T)^T$. With a bit abuse of notation, let $l_2(\Gamma) = l_2(\Lambda, \Theta)$.

Lemma 2. *Suppose that the true parameter Γ_0 has support S . We consider two optimization problems:*

$$\hat{\Gamma} = \arg \min_{\Gamma} \left\{ l_2(\Gamma) + \lambda(\|\Lambda\|_1 + r \|\Theta\|_1) \right\}, \quad (\text{A.14})$$

$$\tilde{\Gamma} = \arg \min_{\Gamma, \bar{S}=0} \left\{ l_2(\Gamma) + \lambda(\|\Lambda\|_1 + r \|\Theta\|_1) \right\}. \quad (\text{A.15})$$

Let $\Delta = \tilde{\Gamma} - \Gamma_0$ and $R(\Delta) = \nabla_{\tilde{\Gamma}}^2 l_2(\Gamma_0) \Delta + \nabla_{\Gamma} l_2(\Gamma_0) - \nabla_{\tilde{\Gamma}} l_2(\tilde{\Gamma})$. If the following conditions hold,

1. the solution $\tilde{\Gamma}$ is unique;
2. $\left\| \left(\nabla_{\tilde{\Gamma}}^2 l_2(\Gamma_0) \right)_{\bar{S}\bar{S}} \left(\nabla_{\tilde{\Gamma}}^2 l_2(\Gamma_0) \right)_{\bar{S}\bar{S}}^{-1} \right\|_{\infty} < 1 - \alpha$ for $0 < \alpha < 1$;
3. $\max\{\|\nabla_{\Gamma} l_2(\Gamma_0)\|_{\infty}, \|R(\Delta)\|_{\infty}\} \leq \frac{\alpha\lambda}{8}$;

then the two ℓ_1 -regularized solutions are identical, $\tilde{\Gamma} = \hat{\Gamma}$.

Proof. Define $\Delta_{\Lambda} = \tilde{\Lambda} - \Lambda_0$, $\Delta_{\Theta} = \tilde{\Theta} - \Theta_0$ and $\Delta = (\Delta_{\Lambda}^T, \Delta_{\Theta}^T)^T$. Let $R(\Delta) = (R_{\Lambda}^T(\Delta_{\Lambda}, \Delta_{\Theta}), R_{\Theta}^T(\Delta_{\Lambda}, \Delta_{\Theta}))^T$ be the residual of second order Taylor expansion of the log-likelihood where

$$\begin{aligned} R_{\Lambda}(\Delta_{\Lambda}, \Delta_{\Theta}) &= \nabla_{\tilde{\Lambda}}^2 l_2(\Lambda_0, \Theta_0) \Delta_{\Lambda} + \nabla_{\Theta} \nabla_{\Lambda} l_2(\Lambda_0, \Theta_0) \Delta_{\Theta} + \nabla_{\Lambda} l_2(\Lambda_0, \Theta_0) - \nabla_{\Lambda} l_2(\Lambda_0 + \Delta_{\Lambda}, \Theta_0 + \Delta_{\Theta}), \\ R_{\Theta}(\Delta_{\Lambda}, \Delta_{\Theta}) &= \nabla_{\tilde{\Theta}}^2 l_2(\Lambda_0, \Theta_0) \Delta_{\Theta} + \nabla_{\Lambda} \nabla_{\Theta} l_2(\Lambda_0, \Theta_0) \Delta_{\Lambda} + \nabla_{\Theta} l_2(\Lambda_0, \Theta_0) - \nabla_{\Theta} l_2(\Lambda_0 + \Delta_{\Lambda}, \Theta_0 + \Delta_{\Theta}). \end{aligned}$$

Following the same arguments as in Lemma 3 in Ravikumar et al. (2011), the ℓ_1 optimization problem (A.14) satisfies

$$\nabla_{\tilde{\Gamma}}^2 l_2(\Gamma_0) \Delta + \nabla_{\Gamma} l_2(\Gamma_0) - R(\Delta) + \lambda Z = 0, \quad (\text{A.16})$$

where $Z = (Z_{\Lambda}^T, Z_{\Theta}^T)^T$ is the sub-differential of the penalty term evaluated at Λ and Θ , and

$$Z_{\Lambda,ij} = \begin{cases} 0 & \text{if } i = j \\ \text{sign}(\Lambda_{ij}) & \text{if } i \neq j \text{ and } \Lambda_{ij} \neq 0 \\ \in [-1, 1] & \text{if } i \neq j \text{ and } \Lambda_{ij} = 0, \end{cases}$$

$$Z_{\Theta,ij} = \begin{cases} r \times \text{sign}(\Theta_{ij}) & \text{if } \Theta_{ij} \neq 0 \\ \in [-r, r] & \text{if } \Theta_{ij} = 0. \end{cases}$$

If we can verify the strict dual feasibility $\|Z_{\bar{S}}\|_{\infty} \leq 1$, then by Lemma 3 in Ravikumar et al. (2011), the restricted solution $\tilde{\Gamma}$ is an optimal solution to the original ℓ_1 problem, i.e., $\tilde{\Gamma} = \hat{\Gamma}$.

Denoting $H = \nabla_{\Gamma}^2 l_2(\Gamma_0)$ and $G = \nabla_{\Gamma} l_2(\Gamma_0)$ for simplicity, the optimality condition of (A.16) in terms of S and \bar{S} can be rewritten as

$$\begin{bmatrix} H_{SS} & H_{S\bar{S}} \\ H_{\bar{S}S} & H_{\bar{S}\bar{S}} \end{bmatrix} \begin{bmatrix} \Delta_S \\ 0 \end{bmatrix} + \begin{bmatrix} G_S \\ G_{\bar{S}} \end{bmatrix} - \begin{bmatrix} R(\Delta)_S \\ R(\Delta)_{\bar{S}} \end{bmatrix} + \lambda \begin{bmatrix} Z_S \\ Z_{\bar{S}} \end{bmatrix} = 0. \quad (\text{A.17})$$

Since H_{SS} is invertible, we have

$$\Delta_S = H_{SS}^{-1}(R(\Delta)_S - G_S - \lambda Z_S). \quad (\text{A.18})$$

Plugging (A.18) back into the second equation in (A.17), we obtain

$$\begin{aligned} Z_{\bar{S}} &= -\frac{1}{\lambda} H_{\bar{S}S} \Delta_S + \frac{1}{\lambda} (R(\Delta)_{\bar{S}} - G_{\bar{S}}) \\ &= -\frac{1}{\lambda} H_{\bar{S}S} H_{SS}^{-1} (R(\Delta)_S - G_S) + H_{\bar{S}S} H_{SS}^{-1} Z_S + \frac{1}{\lambda} (R(\Delta)_{\bar{S}} - G_{\bar{S}}). \end{aligned}$$

Taking the ℓ_{∞} norm of both sides gives

$$\|Z_{\bar{S}}\|_{\infty} \leq \frac{2-\alpha}{\lambda} (\|G\|_{\infty} + \|R(\Delta)\|_{\infty}) + (1-\alpha) \leq \frac{2-\alpha}{\lambda} \frac{\alpha\lambda}{4} + (1-\alpha) < 1.$$

□

Based on Lemma 2, the solution $\tilde{\Gamma}$ is constructed as a witness to the original unrestricted solution $\hat{\Gamma}$. Then $\tilde{\Gamma}$ inherits many optimality properties from $\hat{\Gamma}$, in terms of the discrepancy to the true Γ_0 and the recovery of the signed sparsity pattern. Our next step is to bound the residual term $\|R(\Delta)\|_{\infty}$ in terms of $\|\Delta\|_{\infty}$.

Lemma 3 (Control of remainder). *Suppose that $\|\Delta\|_{\infty} \leq \gamma^{-1} \min\{1/(3C_{\Sigma}), C_{\Theta}/2\}$, then*

$$\|R(\Delta)\|_{\infty} \leq 206 C_{\Sigma}^4 C_{\Theta}^2 C_X^2 \gamma^2 \|\Delta\|_{\infty}^2.$$

Proof. We describe the proof briefly since it follows the same steps as in Wytock and Kolter (2013).

Denote second order Taylor expansion of a function in terms of its differentials

$$\begin{aligned} f(X + \Delta) &\approx f(X) + \text{vec}(\nabla_X f(X))^T \text{vec}(\Delta) + \frac{1}{2} \text{vec}(\Delta)^T (\nabla_X^2 f(X)) \text{vec}(\Delta) \\ &\triangleq f(X) + df(X; \Delta) + \frac{1}{2} d^2 f(X; \Delta). \end{aligned}$$

By the definition of $R(\Delta)$ and the mean value theorem, there exists $t \in (0, 1)$ such that $R_\Lambda(\Delta_\Lambda, \Delta_\Theta) = d(\nabla_\Lambda l_2(\Lambda_0 + t\Delta_\Lambda, \Theta_0 + t\Delta_\Theta); \Delta_\Lambda, \Delta_\Theta)$ and similarly for $R_\Theta(\Delta_\Lambda, \Delta_\Theta)$. As expressions of the above second differentials are tedious, we do not include them here. However, we note that each term in $R_\Lambda(\Delta_\Lambda, \Delta_\Theta)$ and $R_\Theta(\Delta_\Lambda, \Delta_\Theta)$ has a quadratic expression in Δ_Λ and Δ_Θ , with at most four $(\Lambda_0 + t\Delta_\Lambda)^{-1}$ terms, two $(\Theta_0 + t\Delta_\Theta)$ terms and one S_{xx} term. Using the fact that

$$\|ABC\|_\infty \leq \| (C^T \otimes A) \text{vec}(B) \|_\infty \leq \|C\|_1 \|A\|_\infty \|B\|_\infty$$

for any matrices A, B, C and $\|S_{xx}\|_\infty \leq C_X^2$, each term in the second differentials is bounded by

$$C_X \| (\Lambda_0 + t\Delta_\Lambda)^{-1} \|_\infty^4 \| \Theta_0 + t\Delta_\Theta \|_1^2 \| \Delta \|_1^2. \quad (\text{A.19})$$

For an invertible Λ_0 , since $0 < t < 1$, it is easy to verify that

$$(\Lambda_0 + t\Delta_\Lambda)^{-1} = (I + t\Delta_\Lambda \Lambda_0^{-1})^{-1} \Lambda_0^{-1} = \sum_{i=0}^{\infty} (-1)^i (t\Lambda_0^{-1} \Delta_\Lambda)^i \Lambda_0^{-1}.$$

Then

$$\| (\Lambda_0 + t\Delta_\Lambda)^{-1} \|_\infty \leq \| \Lambda_0^{-1} \|_\infty \sum_{i=1}^{\infty} \| \Lambda_0^{-1} \|_\infty^i \| \Delta_\Lambda \|_\infty^i \leq \frac{C_\Sigma}{1 - \gamma C_\Sigma \| \Delta \|_\infty} \leq \frac{3C_\Sigma}{2}.$$

Similarly, since $\| \Delta_\Theta \| \leq \gamma \| \Delta \|_\infty$, we have

$$\| \Theta_0 + t\Delta_\Theta \|_1 \leq \| \Theta_0 \|_1 + \| \Delta_\Theta \|_1 \leq C_\Theta + \gamma \| \Delta \|_\infty \leq \frac{3C_\Theta}{2}.$$

Combining with (A.19), we obtain

$$\|R(\Delta)\|_\infty \leq 206 C_{\Sigma_0}^4 C_\Theta^2 C_X^2 \gamma^2 \| \Delta \|_\infty^2.$$

□

Lemma 4 (Control of Δ). *Suppose that $u \triangleq 2\kappa_H (\max\{\| \nabla_\Theta l_2(\Lambda_0, \Theta_0) \|_\infty, \| \nabla_\Lambda l_2(\Lambda_0, \Theta_0) \|_\infty\} + \lambda) \leq \min\{1/(3C_\Sigma \gamma), C_\Theta/(2\gamma), 1/(412\kappa_H C_\Sigma^4 C_\Theta^2 C_X^2 \gamma^2)\}$. Then*

$$\| \Delta \|_\infty = \| \tilde{\Gamma} - \Gamma_0 \|_\infty \leq u. \quad (\text{A.20})$$

Proof. Recall that $\Delta = \tilde{\Gamma} - \Gamma_0$, $\tilde{\Gamma}_{\bar{S}} = \Gamma_{0,\bar{S}} = 0$, therefore $\|\Delta\|_\infty = \|\Delta_S\|_\infty$. Our goal is to bound the deviation Δ . By (A.18), we have $\Delta_S = H_{SS}^{-1}(R(\Delta)_S - G_S - \lambda Z_S)$. In the following, we use Brouwer's fixed point theorem on a compact set to construct a ball $\mathbb{B}(u)$ that contains Δ . Define the ℓ_∞ -ball $\mathbb{B}(u) = \{\Delta \mid \|\Delta_S\|_\infty < u\}$ and a continuous map $\mathcal{F} : \Delta_S \rightarrow F(\Delta_S)$ such that

$$F(\Delta_S) = H_{SS}^{-1}(R(\Delta_S) - G_S - \lambda Z_S). \quad (\text{A.21})$$

Now it suffices to show $F(\mathbb{B}(u)) \in \mathbb{B}(u)$, as this implies there is a solution to the above equation. By uniqueness of the optimal solution, we can thus conclude that Δ belongs in this ball.

Taking infinity norm to (A.21), we have

$$\|F(\Delta_S)\|_\infty \leq \|H_{SS}^{-1}\|_\infty \|R(\Delta)\|_\infty + \|H_{SS}^{-1}\|_\infty \|G + \lambda Z\|_\infty. \quad (\text{A.22})$$

For any $\Pi \in \mathbb{B}(u)$, by Lemma 3, the first term in (A.22) is bounded by

$$\|H_{SS}^{-1}\|_\infty \|R(\Pi)\|_\infty \leq \kappa_H 206 C_\Sigma^4 C_\Theta^2 C_X^2 \gamma^2 \|\Pi\|_\infty^2 \leq \frac{u}{2}.$$

By the definition of radius u , the second term in (A.22) is bounded by

$$\|H_{SS}^{-1}\|_\infty \|G + \lambda Z\|_\infty \leq \kappa_H (\|G\|_\infty + \lambda) \leq \frac{u}{2}.$$

Therefore, we have $\|F(\Pi)\|_\infty \leq u$. □

Proof of Theorem 1 We first show that $\tilde{\Gamma}$ equals the solution to original objective function (19) $\hat{\Gamma}$ with high probability. Then we proceed with the proof conditioning on this event.

By Lemma 1, we have the element-wise tail conditions for Λ : $\mathbb{P}(\max_{i,j} |\nabla_{\Lambda,ij} l_2(\Lambda_0, \Theta_0)| > \delta) \leq 1/f_\Lambda(n, \delta)$, where $f_\Lambda(n, \delta) = (1/4) \exp(n\delta^2/(3200C_\sigma^2))$, and $\nabla_{\Lambda,ij} l_2(\Lambda_0, \Theta_0)$ denotes the (i, j) -th element in $\nabla_\Lambda l_2(\Lambda_0, \Theta_0)$. For a fixed n , denote

$$\bar{\delta}_{f_\Lambda}(n; \omega) = \arg \max_{\delta} \{f_\Lambda(n, \delta) < \omega\}. \quad (\text{A.23})$$

Similarly, for each fixed $\delta > 0$, denote

$$\bar{n}_{f_\Lambda}(\delta; \omega) = \arg \max_n \{f_\Lambda(n, \delta) < \omega\}. \quad (\text{A.24})$$

By the monotonicity of the function $f_\Lambda(\delta; n)$, it is easy to see that

$$n > \bar{n}_{f_\Lambda}(\delta; \omega) \text{ for some } \delta > 0 \implies \bar{\delta}_{f_\Lambda}(n; \omega) \leq \delta. \quad (\text{A.25})$$

Applying Corollary 1 and Lemma 8 in Ravikumar et al. (2011), for any $\tau > 2$, we have the control of sampling noise for $\hat{\Lambda}$

$$\mathbb{P}\left(\|\nabla_\Lambda l_2(\Lambda_0, \Theta_0)\|_\infty > \bar{\delta}_{f_\Lambda}(n; p^\tau)\right) \leq \frac{1}{p^{\tau-2}} \rightarrow 0 \quad (\text{A.26})$$

where $\bar{n}_{f_\Lambda}(\delta; p^\tau) = 3200C_\sigma^2(\tau \log p + \log 4)/\delta^2$ and $\bar{\delta}_{f_\Lambda}(n; p^\tau) = \sqrt{3200C_\sigma^2} \sqrt{(\tau \log p + \log 4)/n}$. Now we develop the control of sampling noise for Θ . Again, by Lemma 1 we have the element-wise tail probability for $\hat{\Theta}$:

$$\mathbb{P}\left(\max_{i,j} |\nabla_{\Theta, ij} l_2(\Lambda_0, \Theta_0)| > \delta\right) \leq \frac{1}{f_\Theta(n, \delta)}$$

where $f_\Theta(n, \delta) = (1/2) \exp(n\delta^2/(8C_\sigma^2 C_X^2))$.

Define $\bar{\delta}_{f_\Theta}(n; \omega)$ and $\bar{n}_{f_\Theta}(\delta; \omega)$ similarly to (A.23) and (A.24). Applying the union bound over all pd entries of the gradient matrix, we obtain that

$$\mathbb{P}\left(\max_{i,j} |(\nabla_{\Theta, ij} l_2(\Lambda_0, \Theta_0))| > \delta\right) \leq \frac{pd}{f_\Theta(n, \delta)}.$$

Let $\delta = \bar{\delta}_{f_\Lambda}(n; (pd)^\tau)$, then for any $\tau > 1$,

$$\mathbb{P}\left(\|\nabla_\Theta l_2(\Lambda_0, \Theta_0)\|_\infty > \bar{\delta}_{f_\Theta}(n; (pd)^\tau)\right) \leq \frac{pd}{f_\Theta\left(n; \bar{\delta}_{f_\Theta}(n; (pd)^\tau)\right)} = \frac{1}{(pd)^{\tau-1}} \rightarrow 0. \quad (\text{A.27})$$

The last equality follows the fact that $f_\Theta\left(n, \bar{\delta}_{f_\Theta}(n; (pd)^\tau)\right) = (pd)^\tau$, based on the definition of $\bar{\delta}_{f_\Theta}$.

Straightforward calculation shows that $\bar{n}_{f_\Theta}(\delta; (pd)^\tau)$ and $\bar{\delta}_{f_\Theta}(n; (pd)^\tau)$ take the forms

$$\bar{n}_{f_\Theta}(\delta; (pd)^\tau) = 8C_\sigma^2 C_X^2 \left(\frac{\tau \log(pd) + \log 2}{\delta^2}\right)$$

and

$$\bar{\delta}_{f_\Theta}(n; (pd)^\tau) = \sqrt{8C_\sigma^2 C_X^2} \sqrt{\frac{\tau \log(pd) + \log 2}{n}}.$$

Denote $\bar{n}_{f_\Gamma} = \max\{\bar{n}_{f_\Lambda}, \bar{n}_{f_\Theta}\}$, $\bar{\delta}_{f_\Gamma} = \max\{\bar{\delta}_{f_\Lambda}, \bar{\delta}_{f_\Theta}\}$, by (A.26) and (A.27) we have

$$\mathbb{P}\left(\max\{\|\nabla_\Lambda l_2(\Lambda_0, \Theta_0)\|_\infty, \|\nabla_\Theta l_2(\Lambda_0, \Theta_0)\|_\infty\} < \bar{\delta}_{f_\Gamma}\right) \geq 1 - (p^{-(\tau-2)} + (pd)^{-(\tau-1)}). \quad (\text{A.28})$$

Specifically,

$$\begin{aligned}\bar{\delta}_{f_\Gamma} &= \max \left\{ \sqrt{3200C_\sigma^2} \sqrt{\frac{\tau \log p + \log 4}{n}}, \sqrt{8C_\sigma^2 C_X^2} \sqrt{\frac{\tau \log(pd) + \log 2}{n}} \right\} \\ &\leq C_\sigma C_X^* \sqrt{3200} \sqrt{\frac{\tau \log(pd) + \log 4}{n}}\end{aligned}\tag{A.29}$$

where $C_X^* = \max\{C_X^2, 1\}$.

Let \mathcal{A} denote the event that $\max\{\|\nabla_{\Lambda} l_2(\Lambda_0, \Theta_0)\|_\infty, \|\nabla_{\Theta} l_2(\Lambda_0, \Theta_0)\|_\infty\} < \bar{\delta}_{f_\Gamma}$, (A.28) implies that $\mathbb{P}(\mathcal{A}) \geq 1 - (p^{-(\tau-2)} + (pd)^{-(\tau-1)})$. Accordingly, we condition on the event \mathcal{A} in the following analysis.

Next, we verify that the third assumption in Lemma 2 holds. Choose the (larger) regularization penalty $\lambda = (8/\alpha)\bar{\delta}_{f_\Gamma}$, then the first half $\|\nabla_{\Gamma} l_2(\Gamma_0)\|_\infty \leq \alpha\lambda/8$ is satisfied. It remains to establish the bound $\|R(\Delta)\|_\infty \leq \alpha\lambda/8$. We do so by using Lemmas 4 and 3 consecutively. Choose

$$\delta = \frac{1}{2\kappa_H} \left(1 + \frac{8}{\alpha}\right)^{-2} \min \left\{ \frac{1}{3C_{\Sigma}\gamma}, \frac{C_{\Theta}}{2\gamma}, \frac{1}{412\kappa_H C_{\Sigma}^4 C_{\Theta}^2 C_X^2 \gamma^2} \right\},$$

by our choice of λ , the minimum bound on n and the monotonicity property (A.25), we have

$$2\kappa_H \left(1 + \frac{8}{\alpha}\right)^2 \bar{\delta}_{f_\Gamma} \leq \min \left\{ \frac{1}{3C_{\Sigma}\gamma}, \frac{C_{\Theta}}{2\gamma}, \frac{1}{412\kappa_H C_{\Sigma}^4 C_{\Theta}^2 C_X^2 \gamma^2} \right\}.$$

Applying Lemma 4, we conclude that

$$\|\Delta\|_\infty \leq 2\kappa_H \left(1 + \frac{8}{\alpha}\right)^2 \bar{\delta}_{f_\Gamma} \leq 2\kappa_H \left(1 + \frac{8}{\alpha}\right)^2 \bar{\delta}_{f_\Gamma} \leq \frac{1}{\gamma} \min \left\{ \frac{1}{3C_{\Sigma}}, \frac{C_{\Theta}}{2} \right\}.\tag{A.30}$$

Then Lemma 3 gives

$$\begin{aligned}\|R(\Delta)\|_\infty &\leq 206C_{\Sigma}^4 C_{\Theta}^2 C_X^2 \gamma^2 \|\Delta\|_\infty^2 \leq 824C_{\Sigma}^4 C_{\Theta}^2 C_X^2 \gamma^2 \kappa_H^2 \left(1 + \frac{8}{\alpha}\right)^2 \bar{\delta}_{f_\Gamma}^2 \\ &= \left(824C_{\Sigma}^4 C_{\Theta}^2 C_X^2 \gamma^2 \kappa_H^2 \left(1 + \frac{8}{\alpha}\right)^2 \bar{\delta}_{f_\Gamma}\right) \frac{\alpha\lambda}{8} \leq \frac{\alpha\lambda}{8}\end{aligned}$$

where the final inequality follows from the lower bound on sample size n , and the monotonicity property (A.25).

To summarize, we have shown that condition 3 in Lemma 2 holds. Furthermore, a finite C_X implies condition 1, and condition 2 is assumed by the Assumption 3. These allow us to conclude that $\tilde{\Gamma} = \hat{\Gamma}$. By (A.29) and (A.30), the estimator $\hat{\Gamma}$ satisfies the ℓ_∞ bound claimed in Theorem 1(a). Moreover, by the bound (A.20) and the definition of u in Lemma 4, the estimate $\tilde{\Gamma}_{ij}$ cannot differ enough from $\Gamma_{0,ij}$ to change sign when condition (21) is satisfied. This proves Theorem 1(b).

Proof of Corollary 1 Let $\psi = 2\kappa_H(1 + 8/\alpha)C_\sigma C_X^* \sqrt{3200} \sqrt{(\tau \log(pd) + \log 4)/n}$. From Theorem 1, we have $\max \left\{ \left\| \hat{\Lambda} - \Lambda_0 \right\|_\infty, \left\| \hat{\Theta} - \Theta_0 \right\|_\infty \right\} \leq \psi$ with probability at least $1 - (p^{-(\tau-2)} + (pd)^{-(\tau-1)})$. Since Λ_0 has at most $p + s_\Lambda$ non-zeros including diagonal elements and Θ_0 has at most s_Θ non-zeros elements, we have

$$\begin{aligned} \left\| \hat{\Lambda} - \Lambda_0 \right\|_F &= \left(\sum_{i=1}^p (\hat{\Lambda}_{ii} - \Lambda_{0,ii})^2 + \sum_{(i,j) \in E} (\hat{\Lambda}_{ij} - \Lambda_{0,ij})^2 \right)^{1/2} \leq \psi \sqrt{p + s_\Lambda}, \\ \left\| \hat{\Theta} - \Theta_0 \right\|_F &= \left(\sum_{(i,j) \in E} (\hat{\Theta}_{ij} - \Theta_{0,ij})^2 \right)^{1/2} \leq \psi \sqrt{s_\Theta}. \end{aligned}$$

Combining above two inequalities leads to the bound in (22).

Lemma 5. *Suppose that the Assumption 4 holds, then for positive definite matrices $\hat{\Lambda}$ and Λ_0 ,*

$$\begin{aligned} P \left(\lambda_{\min}(\hat{\Lambda}) \geq 0.5C_L \right) &\geq P \left(\left\| \hat{\Lambda} - \Lambda_0 \right\|_F \leq 0.5C_L \right), \\ P \left(\left\| \hat{\Lambda}^{-1} - \Lambda_0^{-1} \right\|_F \leq \frac{2\sqrt{p}}{C_L^2} \left\| \hat{\Lambda} - \Lambda_0 \right\|_F \right) &\geq P \left(\left\| \hat{\Lambda} - \Lambda_0 \right\|_F \leq 0.5C_L \right). \end{aligned}$$

Proof of Lemma 5 This proof is similar to that for Lemma A.1 in Fan, Liao and Mincheva (2011).

Under the event $\left\| \hat{\Lambda} - \Lambda_0 \right\|_F \leq 0.5C_L$, for any vector $\mathbf{v} \in \mathbb{R}^p$ with Euclidean norm $\|\mathbf{v}\| = 1$, we have

$$\mathbf{v}^T \hat{\Lambda} \mathbf{v} = \mathbf{v}^T \Lambda_0 \mathbf{v} - \mathbf{v}^T (\Lambda_0 - \hat{\Lambda}) \mathbf{v} \geq \lambda_{\min}(\Lambda_0) - \left\| \hat{\Lambda} - \Lambda_0 \right\|_F \geq 0.5C_L.$$

The inequality holds by the fact that $\|A\|_2 \leq \|A\|_F$ for any A . Therefore, $\lambda_{\min}(\hat{\Lambda}) \geq 0.5C_L$.

Meanwhile,

$$\begin{aligned} \left\| \hat{\Lambda}^{-1} - \Lambda_0^{-1} \right\|_F &\leq \sqrt{p} \left\| \hat{\Lambda}^{-1} (\Lambda_0 - \hat{\Lambda}) \Lambda_0^{-1} \right\|_2 \\ &\leq \sqrt{p} \lambda_{\min}^{-1}(\hat{\Lambda}) \left\| \hat{\Lambda} - \Lambda_0 \right\|_2 \lambda_{\min}^{-1}(\Lambda_0) \\ &\leq \frac{2\sqrt{p}}{C_L^2} \left\| \hat{\Lambda} - \Lambda_0 \right\|_F. \end{aligned}$$

The first inequality holds because of submultiplicativity of the ℓ_2 norm, and $\|A\|_F \leq \sqrt{p} \|A\|_2$ for any matrix A .

Proof of Theorem 2 Recall that $\text{SKL}(f_0(\mathbf{y}|\mathbf{x}), \hat{f}(\mathbf{y}|\mathbf{x}))$ has an explicit form:

$$\begin{aligned}
& \text{SKL}(f_0(\mathbf{y}|\mathbf{x}), \hat{f}(\mathbf{y}|\mathbf{x})) \\
&= \frac{1}{2} \int_{\mathcal{X}} \mathbf{x}^T U^T \hat{\Lambda} U \mathbf{x} f_0(\mathbf{x}) d\mathbf{x} + \frac{1}{2} \int_{\mathcal{X}} \mathbf{x}^T U^T \Lambda_0 U \mathbf{x} \hat{f}(\mathbf{x}) d\mathbf{x} + \frac{1}{2} \text{tr}(\hat{\Lambda}^{-1} \Lambda_0) + \frac{1}{2} \text{tr}(\Lambda_0^{-1} \hat{\Lambda}) - p \\
&\triangleq I_1 + I_2 + I_3 + I_4 - p,
\end{aligned} \tag{A.31}$$

where $U = \hat{\Lambda}^{-1} \hat{\Theta}^T - \Lambda_0^{-1} \Theta_0^T$. We now derive the upper bound for each of the four terms in (A.31) conditioning on the event $\left\| \hat{\Lambda} - \Lambda_0 \right\|_F \leq 0.5C_L$ and $\left\| \hat{\Lambda}^{-1} - \Lambda_0^{-1} \right\|_F \leq (2\sqrt{p}/C_L^2) \left\| \hat{\Lambda} - \Lambda_0 \right\|_F$.

We first derive an bound for I_1 using the fact that $I_1 \leq 2^{-1} \int_{\mathcal{X}} \left\| \hat{\Lambda} \right\|_2 \left\| U \mathbf{x} \right\|^2 f_0(\mathbf{x}) d\mathbf{x}$. Note that

$$\left\| \hat{\Lambda} \right\|_2 = \left\| \hat{\Lambda} - \Lambda_0 + \Lambda_0 \right\|_2 \leq \left\| \hat{\Lambda} - \Lambda_0 \right\|_2 + \left\| \Lambda_0 \right\|_2 \leq \left\| \hat{\Lambda} - \Lambda_0 \right\|_F + C_U. \tag{A.32}$$

Furthermore, since the Frobenius norm for a vector equals its Euclidean norm, we have

$$\begin{aligned}
\left\| U \mathbf{x} \right\| &= \left\| (\hat{\Lambda}^{-1} \hat{\Theta}^T - \Lambda_0^{-1} \Theta_0^T) \mathbf{x} \right\|_2 \\
&\leq \left\| \hat{\Lambda}^{-1} \hat{\Theta}^T - \Lambda_0^{-1} \Theta_0^T \right\|_2 \left\| \mathbf{x} \right\|_2 \\
&= \left\| (\hat{\Lambda}^{-1} - \Lambda_0^{-1})(\hat{\Theta}^T - \Theta_0^T + \Theta_0^T) + \Lambda_0^{-1}(\hat{\Theta}^T - \Theta_0^T) \right\|_2 \left\| \mathbf{x} \right\|_2 \\
&\leq \left\{ \left\| \hat{\Lambda}^{-1} - \Lambda_0^{-1} \right\|_F (\left\| \hat{\Theta} - \Theta_0 \right\|_F + \left\| \Theta_0 \right\|_F) + \left\| \Lambda_0^{-1} \right\|_2 \left\| \hat{\Theta} - \Theta_0 \right\|_F \right\} \left\| \mathbf{x} \right\|_2 \\
&\leq \left\{ \left\| \hat{\Lambda}^{-1} - \Lambda_0^{-1} \right\|_F (\left\| \hat{\Theta} - \Theta_0 \right\|_F + \left\| \Theta_0 \right\|_F) + \frac{1}{C_L} \left\| \hat{\Theta} - \Theta_0 \right\|_F \right\} \left\| \mathbf{x} \right\|_2 \\
&\leq \left\{ \frac{2\sqrt{p}}{C_L^2} \left\| \hat{\Lambda} - \Lambda_0 \right\|_F (\left\| \hat{\Theta} - \Theta_0 \right\|_F + \left\| \Theta_0 \right\|_F) + \frac{1}{C_L} \left\| \hat{\Theta} - \Theta_0 \right\|_F \right\} \left\| \mathbf{x} \right\|_2
\end{aligned} \tag{A.33}$$

The last inequality holds from Lemma 5. Combined, we have the upper bound for I_1

$$\begin{aligned}
& \frac{1}{2} \int_{\mathcal{X}} \left\{ \left\| \hat{\Lambda} - \Lambda_0 \right\|_F + C_U \right\} \left\{ \frac{2\sqrt{p}}{C_L^2} \left\| \hat{\Lambda} - \Lambda_0 \right\|_F (\left\| \hat{\Theta} - \Theta_0 \right\|_F + \left\| \Theta_0 \right\|_F) + \frac{1}{C_L} \left\| \hat{\Theta} - \Theta_0 \right\|_F \right\}^2 \left\| \mathbf{x} \right\|_2^2 f_0(\mathbf{x}) d\mathbf{x} \\
&\leq (4p) G C_m \left\| \hat{\Lambda} - \Lambda_0 \right\|_F^3 \left\| \hat{\Theta} - \Theta_0 \right\|_F^2,
\end{aligned}$$

where $G = \max\{\int_{\mathcal{X}} \left\| \mathbf{x} \right\|_2^2 f_0(\mathbf{x}) d\mathbf{x}, \int_{\mathcal{X}} \left\| \mathbf{x} \right\|_2^2 \hat{f}(\mathbf{x}) d\mathbf{x}\} \max\{C_U, 1\} \max\{D_T^2, 1\} / \min\{C_L^4, 1\}$ and $C_m = \max\{\int_{\mathcal{X}} \mathbf{x}^T \mathbf{x} f_0(\mathbf{x}) d\mathbf{x}, \int_{\mathcal{X}} \mathbf{x}^T \mathbf{x} \hat{f}(\mathbf{x}) d\mathbf{x}\}$. As the only difference between I_1 and I_2 lies in whether the expectation is calculated with respect to the true or estimated density, this bound also applies to I_2 .

For I_3 , note that

$$\text{tr}(\hat{\Lambda}^{-1} \Lambda_0) = \text{tr}\left((\hat{\Lambda}^{-1} - \Lambda_0^{-1} + \Lambda_0^{-1}) \Lambda_0 \right) \leq \left\| \hat{\Lambda}^{-1} - \Lambda_0^{-1} \right\|_F^2 \left\| \Lambda_0 \right\|_F^2 + p \leq \frac{4p D_L^2}{C_L^4} \left\| \hat{\Lambda} - \Lambda_0 \right\|_F^2 + p,$$

where the first inequality uses the fact that $\text{tr}(A^T B)$ is an appropriate inner product for symmetric matrices A and B , and by the Cauchy-Schwarz inequality, $\text{tr}(A^T B) \leq \text{tr}(A^T A)\text{tr}(B^T B) = \|A\|_F^2 \|B\|_F^2$; and the second inequality holds by Lemma 5 with probability 1. Then

$$I_3 \leq \frac{2pD_L^2}{C_L^4} \left\| \hat{\Lambda} - \Lambda_0 \right\|_F^2.$$

For I_4 , following similar arguments as above,

$$\text{tr}(\Lambda_0^{-1} \hat{\Lambda}) = \text{tr}\left((\hat{\Lambda} - \Lambda_0 + \Lambda_0)\Lambda_0^{-1}\right) \leq \left\| \hat{\Lambda} - \Lambda_0 \right\|_F^2 \left\| \Lambda_0^{-1} \right\|_F^2 + p \leq \frac{p}{C_L^2} \left\| \hat{\Lambda} - \Lambda_0 \right\|_F^2 + p.$$

Then by Corollary 1 and Lemma 5, we have I_1 and I_2 on the order of $\mathcal{O}\left(n^{-5/2}p^{5/2}(\log pd)^{5/2}\right)$, and I_3 and I_4 on the order of $\mathcal{O}\left(n^{-1}p^2(\log pd)\right)$. This proves the claim.

Proof of Theorem 3 The bound of $D(f_0(\mathbf{z}), \hat{f}(\mathbf{z}))$ in (28) comes straightforwardly by combing (25) and (26). However, as the parametric part (25) is conditioning on the event $\left\| \hat{\Lambda} - \Lambda_0 \right\|_F \leq 0.5C_L$, a new lower bound for the sample size n needs to be derived such that this condition is always satisfied. By the RHS of upper bound (22) in Corollary 1, we have

$$n \geq \frac{1600}{C_L^2} \kappa_H^2 C_\sigma^2 32 C_X^2 (p + s_\Lambda) \left(1 + \frac{8}{\alpha}\right)^4 (\tau \log(pd) + \log 4). \quad (\text{A.34})$$

Combining (A.34) with (20) yields (27) after some simple algebra.